A Regional Ground Motion Excitation/Attenuation Model for the San Francisco Region

Luca Malagnini[1], Kevin Mayeda[2], Robert Uhrhammer[3],

Aybige Akinci[1], and Robert B. Herrmann[4]

[1]Istituto Nazionale di Geofisica e Vulcanologia, Rome, Italy

[2]Weston Geophysical Corporation, Lexington, MA

[3]University of California, Berkeley, CA

[4]Saint Louis University, St. Louis, MO

Submitted to: *Bulletin of the Seismological Society of America,*

Manuscript #2006101, Second Revision

October 11, 2006, Version 5.2

Abstract

In addition to providing a location and magnitude, earthquake monitoring efforts are now reporting strong ground motion parameters. In applications such as ShakeMap (Wald et al., 1999), attenuation relationships are used to interpolate between observed values, and efforts are underway to extend the technique to weak-motion as well as strong-motion events. To better define the attenuation relations for weaker motion, we undertake a weak-motion-based ground motion study for the San Francisco Bay Area using 12 stations of the Berkeley Digital Seismic Network (BDSN).

By using small-to-moderate-sized earthquakes located within ~200 km from metropolitan San Francisco, we characterize the scaling of the ground motions for frequencies ranging between 0.25 and 20 Hz, obtaining results for geometric spreading, *Q(f)*, and site parameters using the methods of Mayeda et al. (2005) and Malagnini et al. (2004). The results of the analysis show that, throughout the Bay Area, the average 1-D regional attenuation of the ground motion can be modeled with a bilinear geometric spreading function with a 30 km crossover distance, coupled to an anelastic function $\exp\left(-\frac{\pi f r}{\beta Q(f)}\right)$, where: $Q(f)=180\, f^{0.42}$. A body-wave geometric spreading, $g(r)= r^{-1.0}$, is used at short hypocentral distances ($r < 30$ km), whereas $g(r)= r^{-0.6}$ fits the attenuation of the spectral amplitudes at hypocentral distances beyond the crossover.

The frequency-dependent site effects at the 12 BDSN stations were evaluated in an absolute sense using coda estimated source spectra scaling.

Our results show: i) the absolute site responses, for the frequency band between 0.3 Hz and 2.0 Hz, correlate with independent estimates of the local magnitude residuals (dM_L) for each of the stations; ii) moment-magnitudes (M_W) derived from our path and site-corrected spectra are in excellent agreement with those independently derived using full-waveform modeling and coda-derived source spectra; iii) an empirical, magnitude-dependent scaling was necessary for the Brune stress parameter in order to match the large magnitude spectral accelerations and peak ground velocities with our weak-motion-based model; iv) comparisons at moderate magnitudes (M_W ~5) show that other studies consistently overpredict the high-frequency spectral accelerations; v) structures such as

the velocity contrast across the SAF and the Tertiary basins beneath San Jose and San Pablo Bay do affect ground motions for frequencies higher than 0.33 Hz; we develop a model for the ground motion using BDSN stations that are ideally sited; vi) we use such relationships to predict motions region wide for the Loma Prieta earthquake, well above the maximum magnitude spanned by our data set, on a completely different set of stations. Results compare well with measurements taken at specific NEHRP site classes; vii) the assumption of undisturbed vertical motion, on which the H/V ratio technique is based, is invalid at most sites of the BDSN.

Introduction

A large number of studies are available on predictive relationships for the strong ground motions in California (for an overview, see Abrahamson and Shedlock, 1997). The idea of regionalizing the predictive relationships for the ground motions has been used extensively in different environments: where earthquakes are frequent and data are abundant, like in California (Atkinson and Silva, 2000; Boatwright et al., 2003; or Atkinson and Boore, 1997a, who provided a comparison between recent ground motion relationships in Eastern North America and California), but also where low seismicity rates prevent seismologists from gathering large data sets of strong ground motions, like in some seismic areas located within stable continental regions (e.g., Atkinson and Boore, 1995; Toro et al., 1997). However, most of the effort in the field is obviously focused on studying shallow earthquakes in active tectonic environments to predict strong ground motions for future, damaging earthquakes.

The mentioned studies focus on strong-motion events. However, there is also a need to obtain predictive relationships for weak-motion events that can extrapolate to large events. Here we investigate predictive relationships for peak and spectral ground motion parameters by calibrating regional geometric spreading, frequency dependent Q, and site effects at 12 very broadband stations of the Berkeley Digital Seismic Network. The results of this study are important for the following reasons: i) for providing predictive relationships for the ground motion for small-to-moderate events in the Bay Area, where large-magnitude relationships are already available; ii) for predicting the ground motions

at specific NEHRP site classes; iii) for the possible extrapolations of the results to magnitudes outside the range available in the calibration data set ($M_{wmax} \approx 5.13$). Although directivity can be an important source of variability in observed ground motions (Somerville et al., 1997), such biases are not taken into account in our approach, nor can they be resolved by it. Instead, we make averages over all available azimuths and takeoff angles. For a complete description of the techniques adopted in this study, we refer to the existing literature.

In this study we develop a model for the ground motions in the extended San Francisco Bay Area, and use it to fit the amplitudes of the ground shaking induced by the events of our data set. The model is based on the Brune (1970, 1971) source model, and on the attenuation characteristics of the crust in the region. The latter are quantified after fitting the results of a set of regressions on a data set of weak-motion waveforms. Since our largest event has M_w 5.13, it is correct to state that our model is properly calibrated on small-to-moderate earthquakes. Nevertheless, in order to improve the usefulness of the model, we extrapolate its predictions to M_w 7, and compare our results against recordings of the Loma Prieta earthquake. Extrapolations are obtained through the calibration of the stress parameter of the Brune source spectrum, which we need to increase as magnitude increases. Based on results taken from Boore and Joyner (1997), all predictions are adjusted to specific NEHRP site classes. Finally, we compare our weak-motion-based model, between M_w 5 and M_w 7, to a reference model for the region (Atkinson and Silva, 2000). The results of this study are relevant for real-time applications such as ShakeMap, where accurate (not conservative) predictions of the amplitudes of the ground motions for moderate earthquakes are needed.

Most of the results of this study are based on the assumption that the area under investigation is homogeneous in terms of the main characteristics of the wave propagation (see also Malagnini et al. 2000a,b, 2002, 2004; Malagnini and Herrmann, 2000; Akinci et al., 2001, 2006; Scognamiglio et al., 2005; Morasca et al., 2006; Bodin et al., 2004). In other words, we assume that at wavelengths corresponding to the frequency range between 0.25 and 20 Hz, there are no important variations in the gross structure of the crust around the Bay Area, especially for its upper part, and the limited lateral extent of the studied region (within 150-200 km from metropolitan San Francisco) makes such

hypothesis more reasonable. However, it should be noted that the same assumption is implicitly made in most, if not all, strong motion studies.

A Reference Model for the Ground Motion in California

The study by Atkinson and Silva (2000), hereinafter referred to as AS2000, was chosen as a reference and will be compared against our predictions. Although there are many different models, this one was chosen because it is widely used as a reference, and comparisons with other models can be done in a relative fashion. The magnitude of validity for the AS2000 relationships is between M_w 4 and 8, and thus overlaps the magnitude range of our study. A more exhaustive comparison of the model developed in this study and other published results is beyond the scope of this paper.

The characteristics of the spectra radiated by different source models play a major role in the predictive relationships for large events at low frequencies. Some authors (Atkinson and Boore, 1997b; Schneider et al., 1993; Silva and Darragh, 1995; Atkinson and Silva, 1997) pointed out the tendency of the Brune (1970, 1971) spectral model to overpredict low-frequency spectral amplitudes of large earthquakes. It has been shown, however, that when used in conjunction with a stochastic model (Hanks and McGuire, 1981; Boore, 1983; Boore et al., 1992; Silva and Darragh, 1995), the Brune source spectrum with a stress parameter $\Delta\sigma$=5-10 MPa provides reasonable results in predicting the high-frequency ground motions (the stress parameter trades-off with the attenuation at high-frequency). Boatwright and Choy (1992), and Atkinson and Boore (1997b) observed that a two corner-frequency spectral model seems to better predict the spectra of large intra-plate events, which generally depart from the Brune model. One feature of the AS2000 model is that it assumes a source model of a spatial point-source with two corner frequencies. In this study, instead, we use a single corner frequency model.

The Data Set

We compiled a data set of 5769 waveforms from 281 events recorded at either 80 sps or 100 sps by the Berkeley Digital Seismic Network (BDSN). Figure 1 shows a map of the region, with the locations of the events used for this study, and of the BDSN stations that are in our data set. Figure 2 shows the distribution of the data with respect to

the hypocentral distance at each station. Except for station PACP, the distributions are relatively even. Data used in this study are those from the *HH* data streams (80 sps or 100 sps) and the maximum frequency that we consider is 20 Hz.

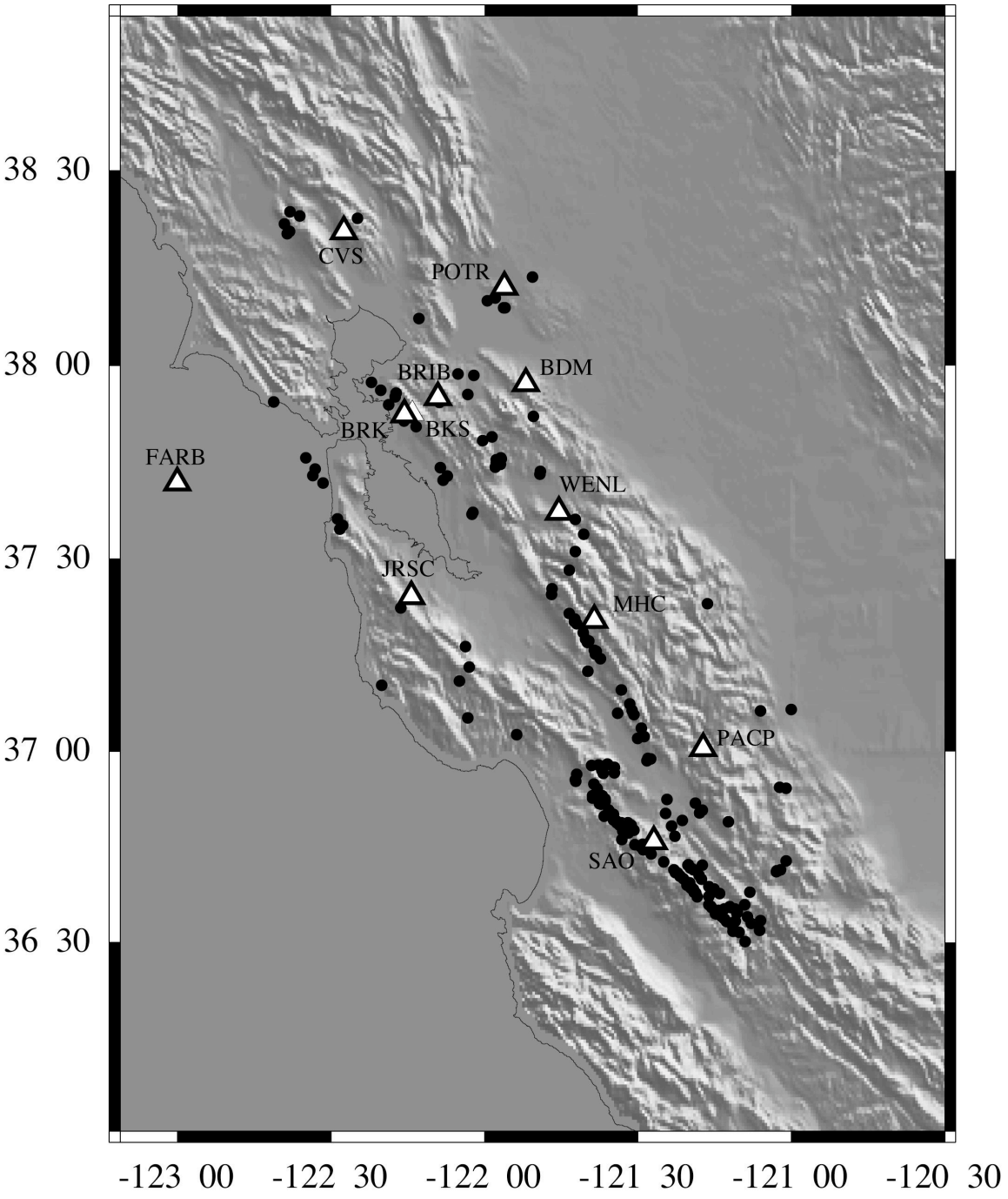

Figure 1. Map of the region along with the events used for the regressions, and the 12 BDSN stations used in this study.

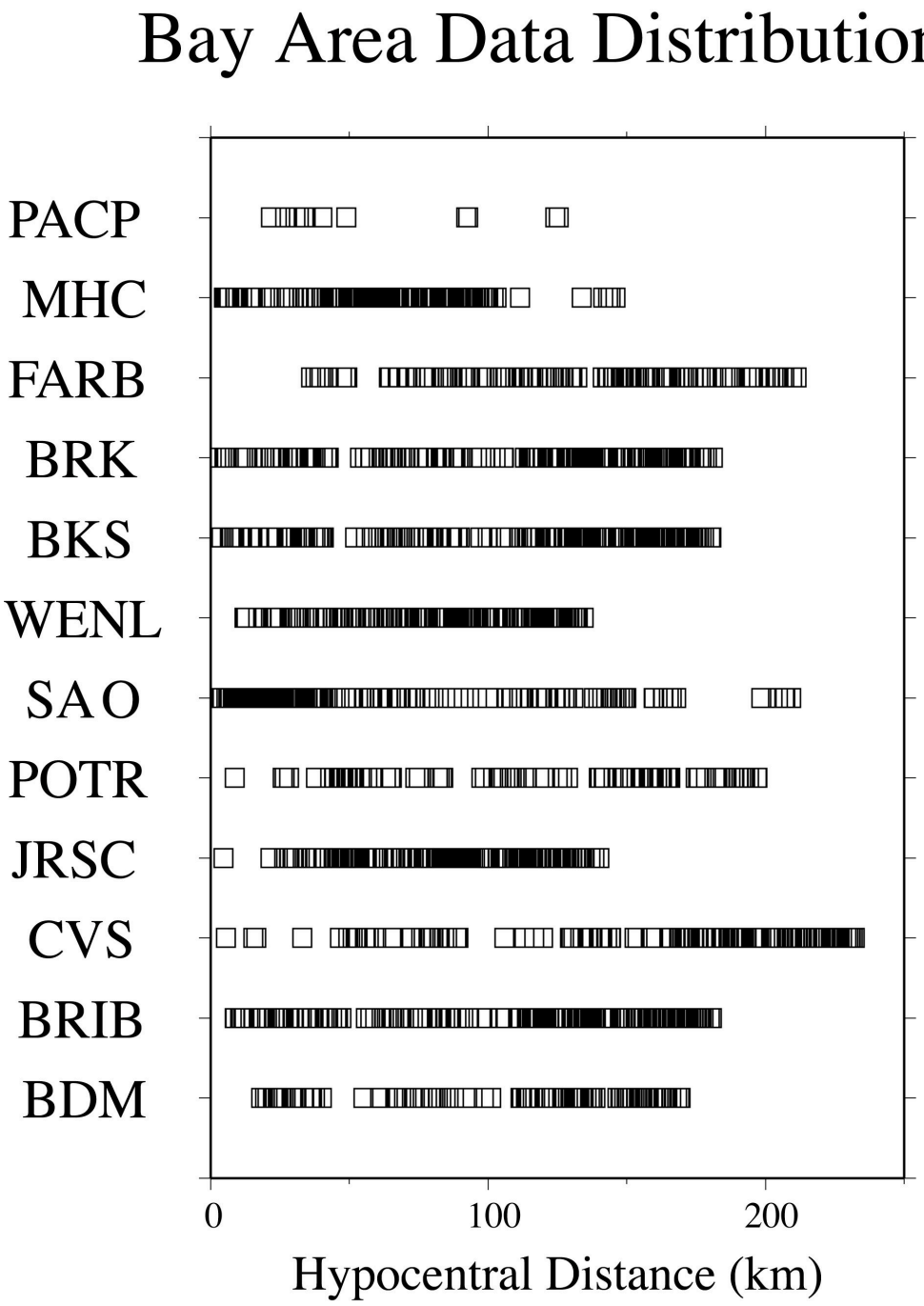

Figure 2. For each station we plot the distribution of sampled hypocentral distances. Except for the station PACP, the distributions of sampled distances at the other stations are very even, and guarantees that the results are reliable for the entire distance range.

Modeling

Duration of the ground motion

Random Vibration Theory (RVT, see Cartwright and Longuet-Higgins, 1956) is used to quantity the different time-domain parameters that characterize the ground motions in a specific region. To accomplish this, we need to quantify the effective duration of the ground motions as a function of frequency and hypocentral distance. In order to make specific predictions for large earthquakes, the duration of the event must be added in the form of a constant term equal to the inverse of the corner frequency.

A unique definition of the effective duration of the ground motions is not available. For example, Boatwright and Choy (1992) defined it as the sum of two terms, the inverse of twice the lowest spectral corner frequency, and the length of the dispersion window due to the crustal propagation. Atkinson (1993) quantified the duration of the ground motions in Eastern North America between 10 and 1000 km from the hypocenter, observing a distance range (60-250 km) for which duration was almost constant. Similar conclusions were reached by Toro and McGuire (1987), who used a constant duration function for moderate and large earthquakes: $T=1/f_0$, for hypocentral distances less than 100 km.

Our definition of effective duration for the ground motions is that given by Raoof et al. (1999) and corresponds to the time window that comprises between 5% and 75% of the integrated energy. Such a quantity is computed at each sampling frequency, for each recorded seismogram, and a piece-wise-linear functional form is found by regressing all the available data points.

In general, the duration of the ground motions is affected by the crustal structure at the regional scale. For example, depth clusters determine multi-modal distributions (as in the northeastern Alps, see Malagnini et al., 2002). Duration at low-frequency ($f<1.0$ Hz), generally increases with distance. Past the location of the first strong supercritical reflections, duration of the ground motions may increase more rapidly with distance (Herrmann and Malagnini, 2005). High-frequency duration tends to increase less rapidly with distance, perhaps due to the dominance of a single S-arrival instead of an ensemble of arrivals, sometimes being almost constant over most of the available distance range.

The effect of Q may also explain this phenomenon.

For each sampling frequency, and each filtered seismogram, the 5%-75% duration was automatically computed. Results are plotted in the various frames of Figure 3. L_1-norm optimizations were run in order to obtain piecewise-linear functions to quantify the median values of the duration distributions at different hypocentral distances. Although a clear functional form was not obtained for the lowest frequencies (0.25 Hz and 0.6 Hz), reliable durations were computed for all the other central frequencies. Even between 0.25 Hz and 0.6 Hz, the quantities shown in Figure 3 show an acceptable median behavior, and can be used in the RVT applications. The frequency dependence of the empirical duration functions of Figure 3 will be taken into account in all the ground motion predictions provided in this study. The median values of duration computed at each sampling frequency are provided in Tables A1a,b, in Appendix 1.

Throughout this study, when peak ground motions are predicted (PGA, PGV), the 1.75 Hz duration function is used. The 1.75 Hz central frequency was chosen in order to reach a compromise that could be used for both PGA's and PGV's, which are carried, at different distances, by waves of different dominant frequencies. This issue is not a critical one: even if a factor of two affected the estimate of duration used for computing PGA's at short distance, so that the "right" duration was a factor of two smaller, this would result in a final estimate of the PGA only a factor of $\sqrt{2}$ smaller than what it should be. When the PSA's were computed at different central frequencies, we used the duration function specific for each frequency.

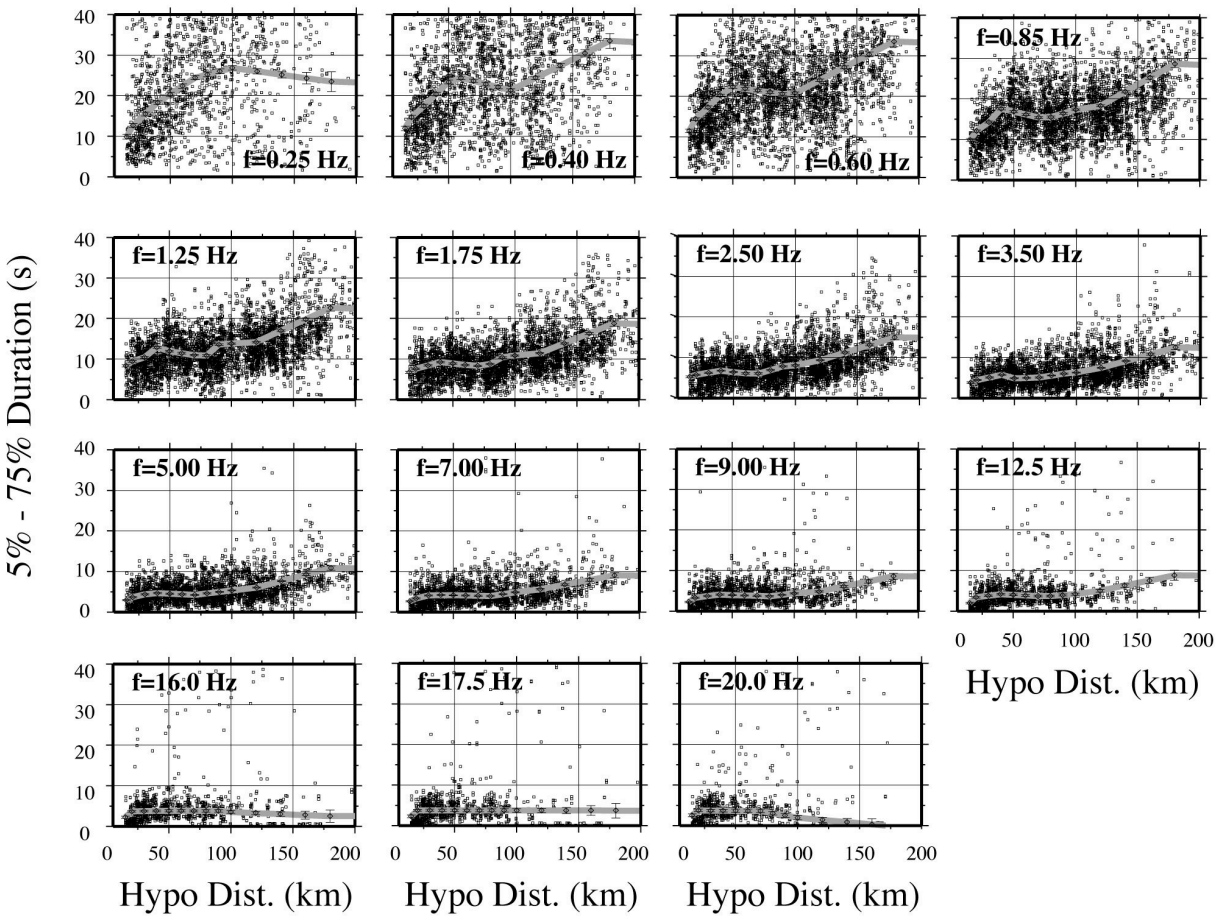

Figure 3 – 5%-75% duration of the ground motion, computed for each filtered seismogram, plotted as a function of the hypocentral distance. The thick gray lines linking the symbols with the y-axis error bars represent L_1-norm estimates of piece-wise linear functions describing the duration. The values of duration plotted in the Figure are also listed in Tables 1a,b.

Amplitudes of the Ground Motion

The analysis of both spectral and time domain amplitudes is not strictly necessary (e.g., Fourier amplitudes in the frequency domain, and peak amplitudes of the bandpass filtered waveforms in the time domain). However, by considering both, we were able to model the peak values and the Fourier amplitudes with the same calibration parameters, thus producing an internally self-consistent model for the excitation and propagation of the ground motion at regional distances. In the following, we will show only the results

of the peak values analysis, but every step of the processing was carried out also in the frequency domain.

Peak values from the narrow bandpass filtered waveforms, and the rms-averages of the Fourier amplitude spectra, were separately regressed in a simple scheme to obtain excitation, regional propagation, and site terms at every sample frequency (see Raoof et al., 1999; Malagnini et al., 2002). Figure 4 shows the regional attenuation terms, normalized to zero at the reference hypocentral distance of 40 km. For plotting purposes only, these empirical functions are also normalized to a reference body-wave-like decay, so that a horizontal line in Figure 4 would decay proportionally to 1/r. The colored lines represent the results of the regressions (note the error bars at the distance nodes), whereas the black lines in the background represent our theoretical predictions based on a bi-linear geometric spreading function (in the log-log space) with a 30 km crossover distance, coupled to an exponential function, $\exp(-\pi f/\beta Q(f))$, where $Q(f)=180f^{0.42}$ is the crustal quality factor. A body-wave-like geometric attenuation ($g(r)=1/r$) is used to model the decay of the Fourier amplitudes at short distances (all frequencies), and a surface-wave-like decay, ($g(r)=r^{-0.6}$), fits the results at larger hypocentral distances. Equation (1) represents the functional form used for the logarithmic crustal propagation term (D), normalized to the arbitrary reference hypocentral distance r_{ref}=40 km.

$$D(r,r_{ref},f)=\log_{10}\left[\frac{g(r)}{g(r_{ref})}\right]-\left[\frac{\pi f}{\beta Q_0 f^{\eta}}(r-r_{ref})\right]\log_{10}e \qquad (1)$$

Compared to the set of parameters that was published by Raoof et al. (1999) for Southern California, the numbers obtained for the extended Bay Area are equivalent. However, we must point out that the frequency-dependent duration function used in this study for predicting peak values at regional distances is very different, for some frequency-hypocentral distance pairs, from the duration function $T(r)=T_0+0.05r$ (r in km) that was used by Raoof et al. (1999) (and by AS2000).

Changes in the geometric spreading may correspond to the arrivals of supercritical bounces off primary crustal interfaces. Atkinson and Boore (1997) point to the recordings of the 1988 Saguenay (Québec) earthquake as good examples of the effects of supercritical bounces around 100 km from the source. Similarly, the 30-km

crossover distance described in this study must be related to some strong (upper) crustal interface.

The fact that well-developed surface waves seem to dominate the seismograms starting at relatively short distance is consistent with relatively low, shallow crustal S-wave velocities in the region around the Bay Area. From Figure 3, it seems that a change in slope affects a number of duration functions near 80-100 km (e.g., 0.85 Hz, and 1.75 Hz). Near-receiver multiple phases in this distance range may also contribute significantly to the duration. Examples of these phases are in Dreger and Helmberger (1990) and Baise et al. (2003). These near-receiver, shallow interfaces (upper 4 to 5 km) appear to be a quite common characteristic of local distance waveforms.

Random Vibration Theory (RVT), based on the duration information shown in Figure 3 and on the described geometric/anelastic attenuation function (Equation 1), is used to produce the synthetic attenuation lines that are plotted in black in Figure 4. The same attenuation model (geometric and anelastic) is used to match the Fourier Amplitude D(r) (not shown). No information on duration is needed in the modeling of the Fourier spectral amplitudes.

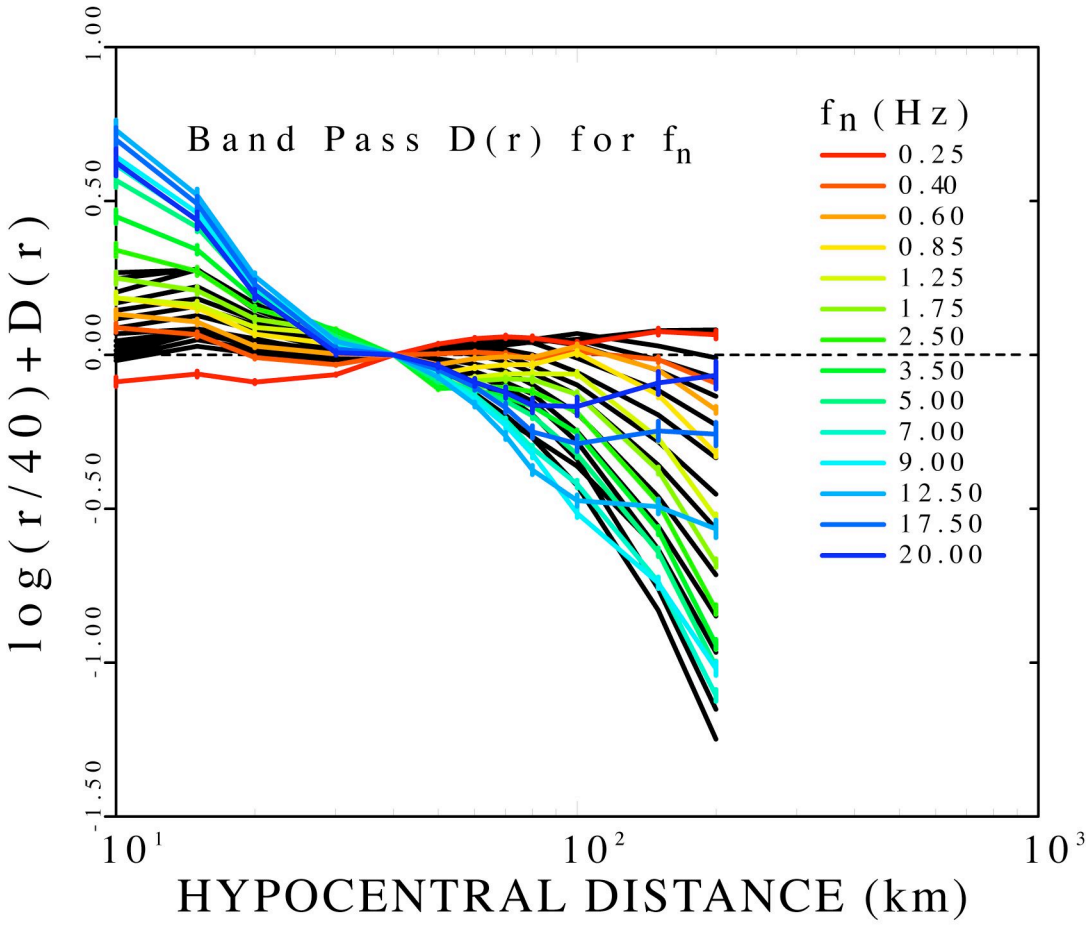

Figure 4 –Empirical regional attenuation terms for the peak filtered amplitudes (colored lines). The black lines in the background represent the frequency-dependent synthetic RVT predictions of the empirical D(r,f) function, normalized to zero to the arbitrary reference hypocentral distance of 40 km. For these predictions, we used the attenuation model described in the text, (the same one used for the Fourier amplitudes), and all the frequency-specific estimates of duration presented in Figure 3. High-frequency empirical curves (f > ~10 Hz) depart from their predicted trends at around 80 km hypocentral distance, when the peak amplitudes are no longer carried by direct waves. Note that, for plotting purposes only, the curves are normalized to a 1/r decay (the horizontal line in this picture represents a decay ~ 1/r).

Figure 5 shows the empirical excitation terms obtained through the regressions of the filtered peak amplitudes, for which RVT was used. Superimposed on the empirical terms are the synthetic excitation terms at various magnitudes. They were obtained by combining the Brune spectral model, the regional geometric/anelastic attenuation just defined for the regional propagation terms, and the assumed absolute empirical site term at the 35 m-deep borehole station BRIB, which was arbitrarily chosen as the reference for

the regressions. The choice of the reference station was implemented by forcing the average of the BRIB horizontal site terms to be null at all frequencies. In the next section of this paper, we will show that station BRIB, from 0.25 Hz to 2.0 Hz, behaves very closely to a 'Generic Rock Site' in the Boore and Joyner (1997) sense, coupled with an attenuation term with a parameter κ_0=0.055 sec. In general, excitation terms need to be calibrated against independent estimates of M_w to ensure that the absolute amplitudes are correct.

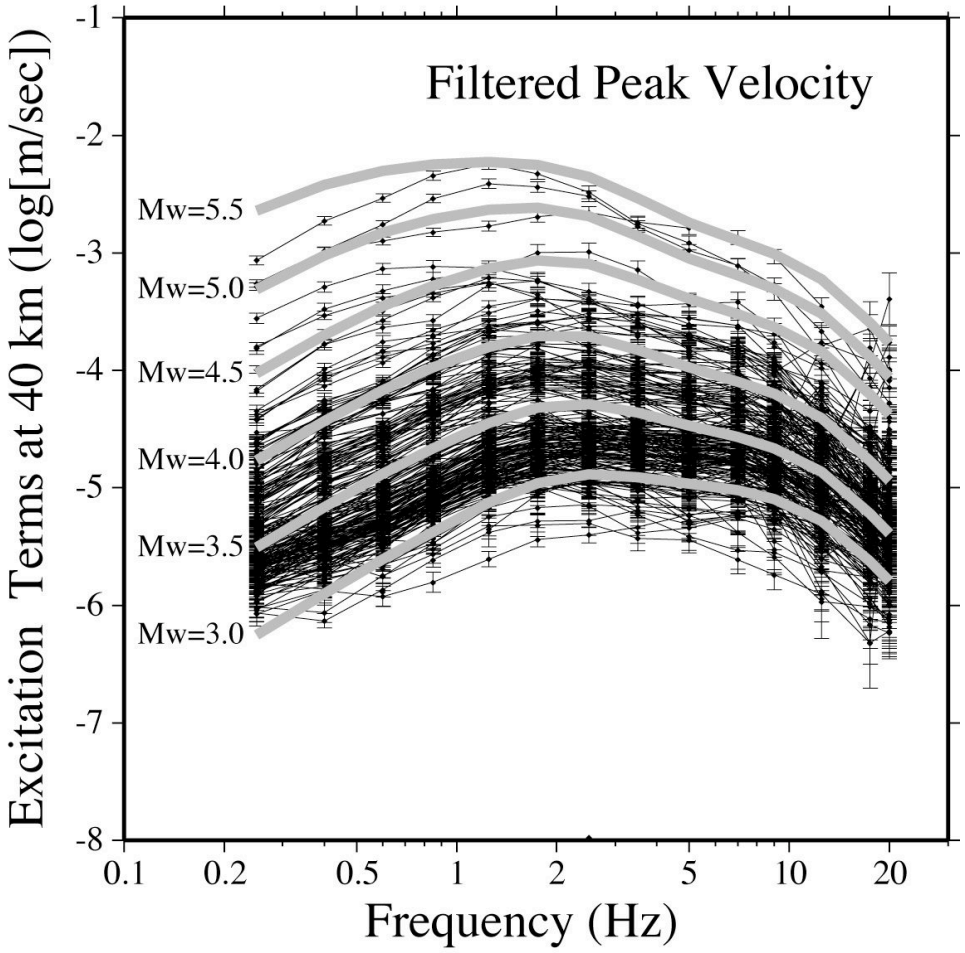

Figure 5 – Excitation terms from the regressions of the filtered peak ground velocities (horizontal ground motion). Black lines connecting symbols with y-axis error bars represent the empirical terms. Thick gray lines represent the theoretical terms computed via a Brune spectral model, coupled to the geometric-anelastic attenuation model described in the text. The frequency-specific estimates of duration at the different frequencies, at the 40 km reference hypocentral distance, are used for the RVT simulations of the filtered peak ground velocities. Equivalent fits characterize the Fourier ground velocity excitation terms (not shown).

Estimating Absolute Site Terms

The moment-rate source spectra used in this study are those computed by

Mayeda et al. (2005), who used a new technique to take into account the lateral variations of the propagation properties of the crust in California. The technique allowed for the computation of precise moment-rate spectra derived from coda envelopes, which were unbiased by the effects of lateral heterogeneities.

Figure 6 shows the coda-derived source terms that were used to compute the absolute site responses. They were transformed to velocity spectra, then the regional geometric/anelastic attenuation function, $g(r)*\exp(-\pi f\, r / \beta Q(f))$, was used to simulate the regional propagation to the reference hypocentral distance, 40 km. The attenuated absolute spectra shown in Figure 6 were used to infer the absolute behavior of the sites used in this study. Source spectra are indicated as $EXC_j(f,r=r_{ref})$ in the matrix form in equation (2).

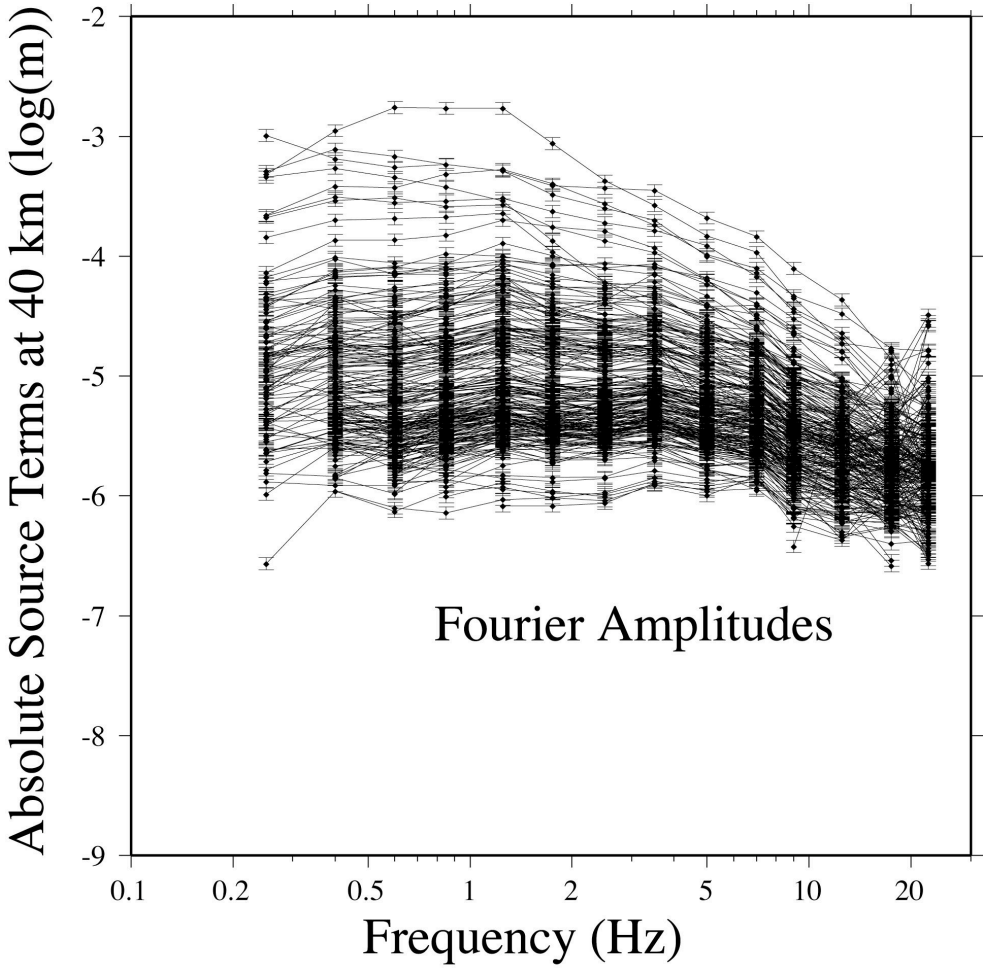

Figure 6 – Absolute source terms from the moment-rate spectra independently estimated using the coda calibration parameters from Mayeda et al. (2005). For the present plot, the moment-rate spectra were transformed to velocity spectra, then the regional attenuation function $g(r)*\exp(-\pi f r / \beta Q(f))$ was used to

simulate the regional propagation to a hypocentral distance of 40 km.

Let $a_k(r_{ij},f)$=k-th observation (i.e., the Fourier spectral amplitude around frequency f, recorded at the hypocentral distance r_{ij}):

$$\log_{10}(a_k(r_{ij},f))=EXC_j(r=r_{ref},f)+SITE_i(f)+D(r_{ij},r_{ref},f) \qquad (2)$$

the term $D(r_{ij},r_{ref},f)$, described in (1), is the one obtained in the regression section (see Figure 4), and so the $SITE_i(f)$ are the only unknowns. Since the empirical excitation terms by Mayeda et al. (2005) are not biased by any specific site term, and the effects of the regional attenuation of Figure 4 were uniquely isolated, the site terms obtained with these regressions are unique and 'absolute'. Figure 7 shows the absolute site terms for the three components of the ground motion, as they are obtained from the inversion of equation (2), at all the stations used in this study. Such terms are called "absolute" because they represent the response of whatever is not included in the average regional path terms, i.e., the absolute response from the surface to the depth of a bedrock common to all sites, where they all can be considered equivalent. Due to the nature of the regression method, such quantities are averaged over all the sampled azimuths and incidence angles.

Figure 8 shows that, as anticipated in the previous section, up to 2 Hz, our 35 m-deep borehole reference station (BRIB) behaves like the "Generic Rock Site" defined by Boore and Joyner (1997). The high-frequency roll-off at BRIB can be described by a parameter κ_0=0.055 sec, superimposed on the same Generic Rock Site by Boore and Joyner (1997). A very similar roll-off characterizes CVS, JRSC, POTR, PACP. A steeper decay characterizes the site terms at high-frequency at BDM, BKS, MHC, and WENL. In most cases, with the exception of BRK and FARB, both the vertical and the horizontal ground motions are affected by significant distortions induced by the shallow geology.

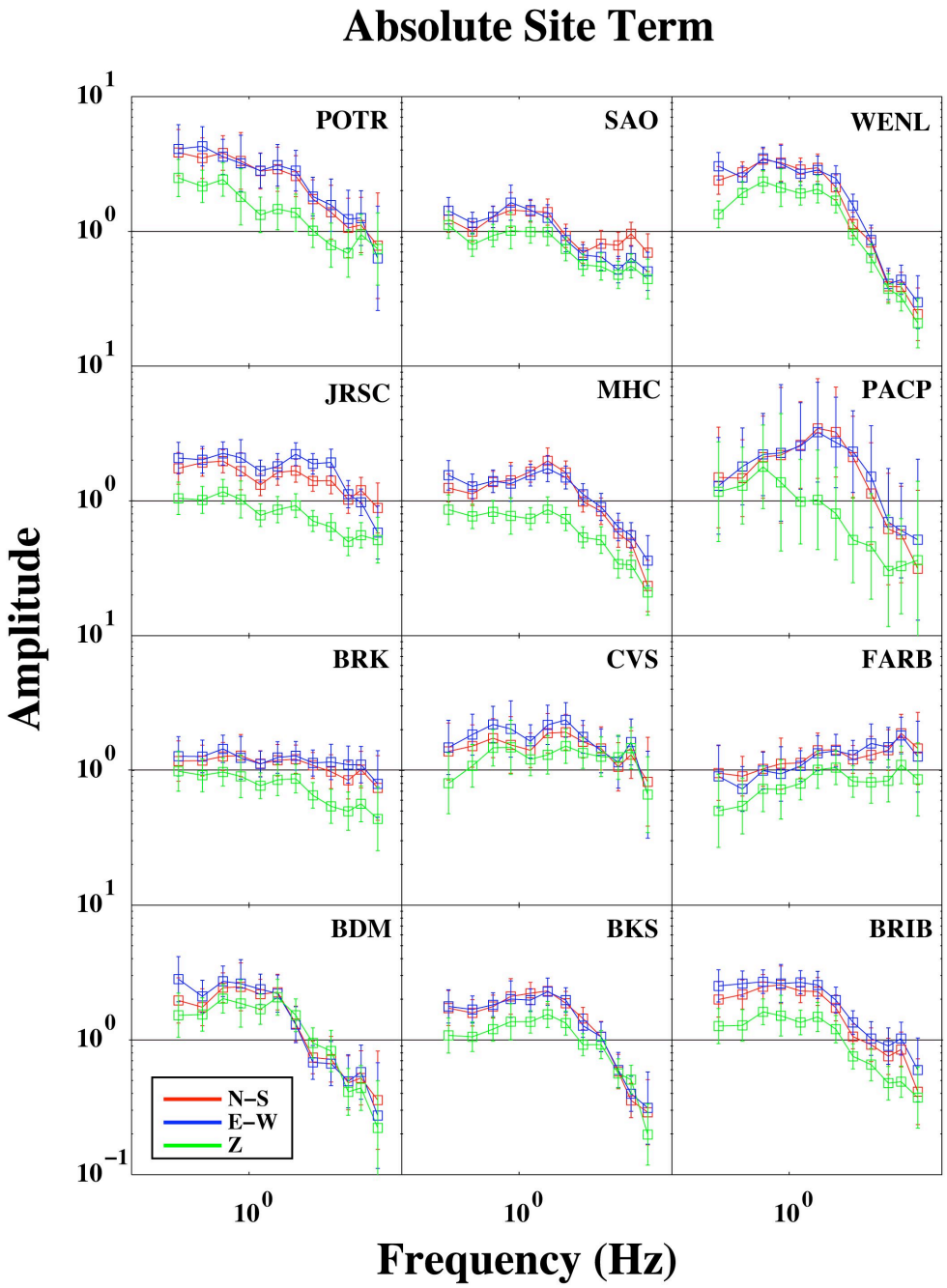

Figure 7 – Absolute site terms of stations BDM, BKS, BRIB, BRK, CVS, FARB, JRSC, MHC, POTR, SAO, WENL, and PACP (N-S component, red, E-W component, blue, vertical, green).

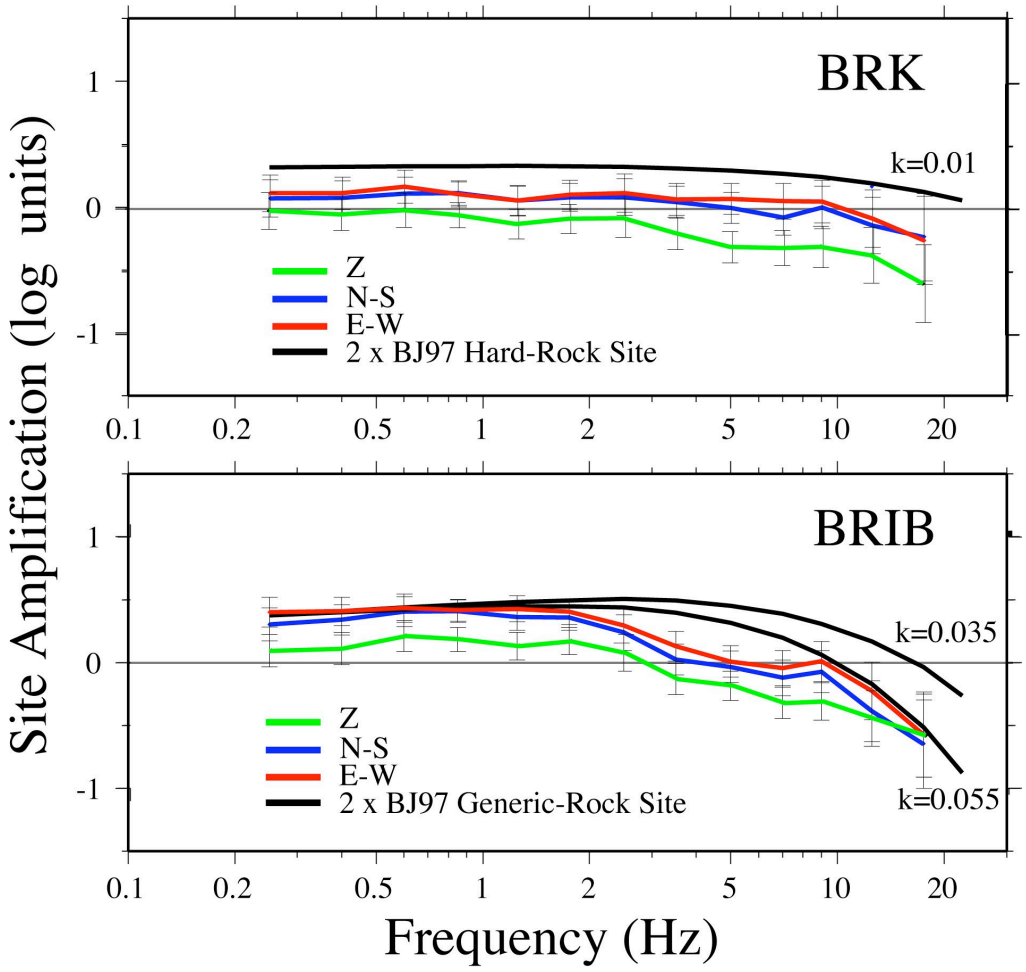

Figure 8 – Absolute site terms of stations BRK, and BRIB (N-S component, red; E-W component, blue; vertical, green). Station BRK is located on Jurassic/Cretaceous Franciscan sandstone. The instruments at BRK are sited in the sub-basement of a 4-story building on the UC Berkeley campus. For BRK, we compare its absolute site terms with the hard-rock site term by Boore and Joyner (1987), coupled with the anelastic attenuation parameter k=0.01 sec. The site terms at station BRIB are compared with the generic rock site term by Boore and Joyner (1997) (black lines), coupled with two different shallow anelastic attenuation terms. The value of k=0.035 sec is the one recommended by Atkinson and Silva (2000), whereas the high-frequency roll-off at site BRIB is best described by k=0.055 sec. At BRIB, located on sandstone, the Guralp CMG-3T seismometer of the BDSN is installed at a depth of 35 meters.

Correlation of Absolute Sites with Local Magnitude Station Adjustments (δM_L)

Independently determined magnitude residuals can be used to compare against the absolute site terms. Local magnitude residuals were computed for all the stations used in this study. All the magnitude residuals, -δML(H) (N-S and E-W), and -δML(V) (vertical) are plotted in different colors in Figure 9. The visual inspection of the eight frames indicate that, although all the frequencies up to 2.5 Hz show a good degree of correlation,

the linear trend of the data set of 1.25 Hz is characterized by the best linear correlation (1.25 Hz is the corner frequency of the Wood-Anderson seismometer). This is in good agreement with the value of the median dominant frequency on which the ML's are computed (f_d=1.3± 0.3 Hz). The central frequency of 1.75 Hz also shows an excellent correlation. The results shown in the figure are similar to the ones described by Mayeda et al. (1991), who performed a similar analysis on coda-based spectral measurements. The data points of the best frequency (1.25 Hz) are quantified in Table A2.1. Correlation deteriorates beyond 2 Hz, and finally breaks down at f=3.5 Hz. Higher sampling frequencies (not shown in this picture) show no correlation at all. For the details of the computation of the magnitude adjustments, the reader is referred to Appendix 2.

L-1 Bilinear Regression: y=mx+b
Max Err on Site Term=0.20 (HHZ HHN HHE)

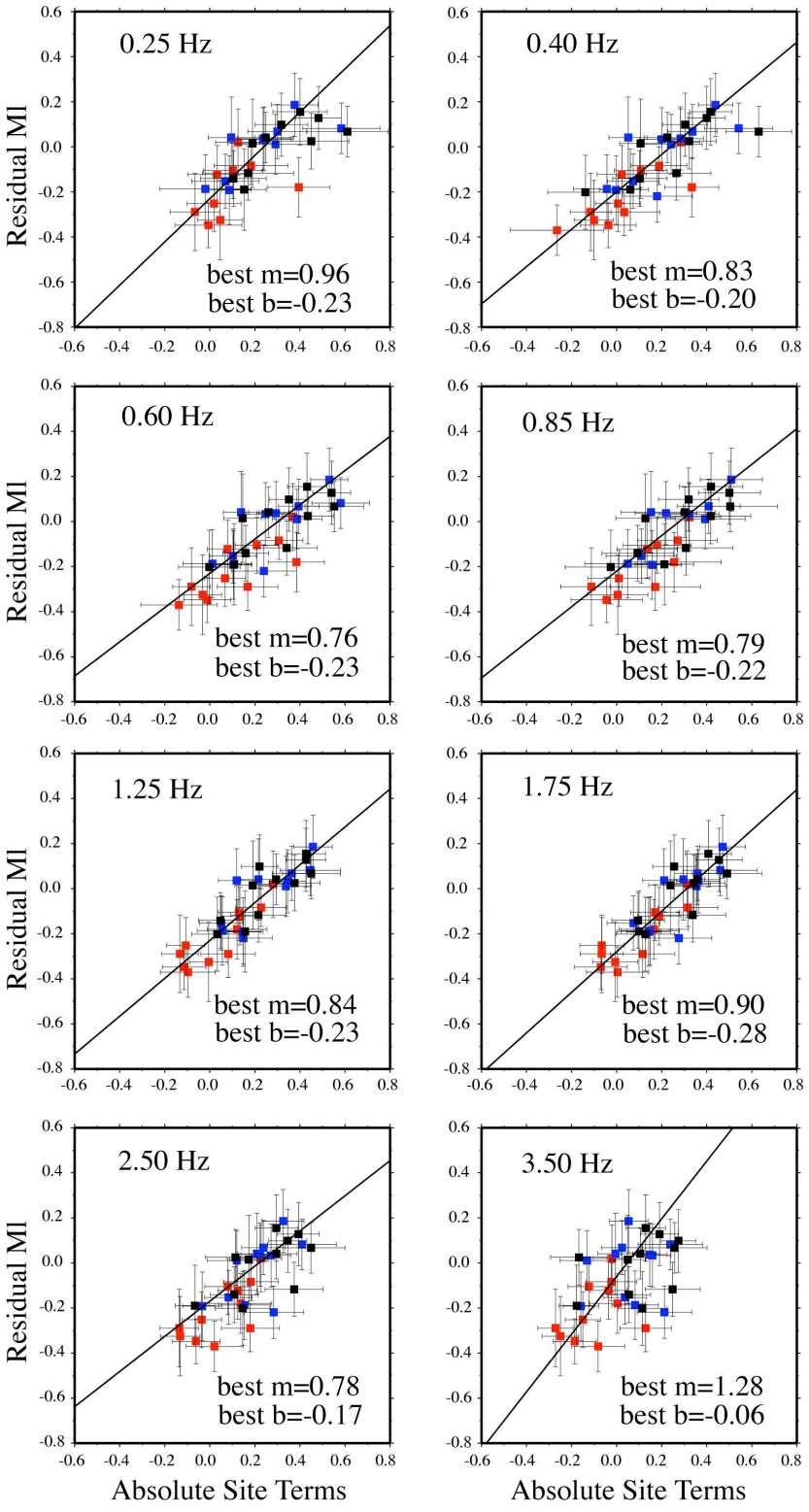

Figure 9. Correlation between the absolute site terms obtained at some of the central sampling frequencies, and the M_L residuals (not a function of frequency). M_L residuals were obtained by multiplying the M_L adjustments of Table A2.1 by –1. Each frame shows all the data points with error bars on both the x- and y-axes. A bilinear regression is performed, in the L-1 sense, at each central frequency. The best parameters of the linear functions are indicated for each frequency. Note: PACP was not included due to lack of data. The colors indicate the component of the ground motion, as explained in the picture's title.

Calibrating Magnitudes

In order test our spectral attenuation model, we used it to reproduce the accurate low-frequency amplitudes of the moment-rate spectra obtained by Mayeda et al. (2005) for each earthquake of our data set. We did so by correcting the observed spectra for the attenuation experienced along the entire wave paths, after integrating the crustal attenuation with the absolute site response of each component of the ground motion. In Figure 10 we compare the estimates of M_W obtained in this study with those by Mayeda et al. (2005). We consider the coda-wave moment magnitudes as "ground-truth", as these were shown to match those derived from full-waveform inversions from the U.C. Berkeley's moment-tensor catalog (see Pasyanos et al., 1996, and the UCB MT catalog: http://seismo.berkeley.edu/~dreger/mtindex.html).

The parameters used to compute the scalar moments from the low-frequency direct-wave spectral amplitudes were the following: $<R_{\theta\varphi}>=0.55$ (rms-averaged radiation pattern); $\beta=3.5$ km/sec; $\rho=2.8e+03$ kg/m^3; $F=2$ (free surface effect); $FF=0.707$ (coefficient of partition of energy). The function used to define the length of the S-wave time windows was one-half of the 1.75 Hz duration function of Figure 3 (Approximately, $T(r,f=1.75Hz)=const=7$ sec for $r \leq 70$ km, and $T(r,f=1.75Hz)=0.01*r$ for $r > 70$ km, r in km). Time window lengths were also augmented by the quantity $T_0=1/f_0$, the duration of the rupture, inferred from an estimate of M_L computed on the fly. The geometric spreading was: $g(r)=r^{-1.0}$ for $r \leq 30$ km, and $g(r)=r^{-0.6}$ beyond that hypocentral distance.

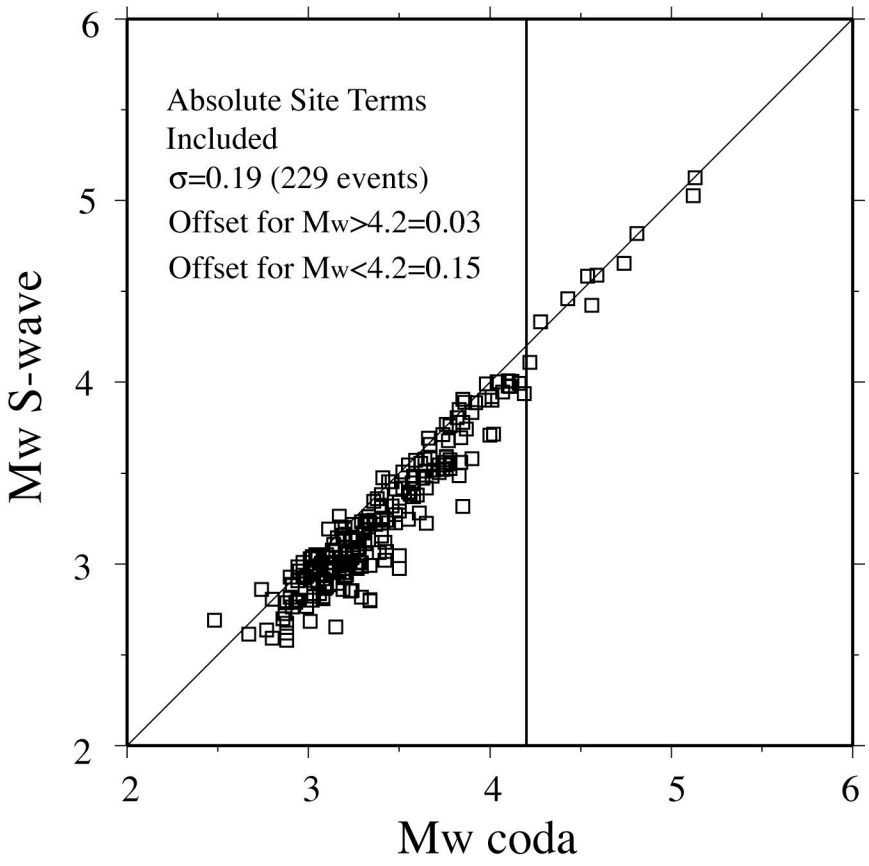

Figure 10: The results shown above were obtained using the code developed by Bodin et al. (2004) for the automatic computation of the moment magnitude, given g(r), Q(f), κ_0, and T(r) obtained from the regional study on excitation and attenuation of the ground motion. The attenuation model is given in Equation (1), with the geometric spreading and the parameter Q(f) described in the text.. Other parameters in the code are listed in the text. Duration used is the one at 1.75 Hz (T=const.=7 sec for r<70 km; T=0.01*r for r>70 km, r in km). The coda-wave moment magnitudes represented our reference estimates. Y-axis: automatically obtained S-wave M_w's, computed by correcting the observed spectra for the regional attenuation (path and absolute site terms), X-axis: "ground-truth", coda-based M_w's, computed by Mayeda et al (2005). A residual adjustment of 0.03 magnitude units would be needed to perfectly match (in an L-1 sense), the ground-truth values. For smaller magnitudes (M_w<4.2), scatter is larger and a residual adjustment of 0.15 magnitude units is found.

Predicting the Ground Motion

Once the path and absolute site effects were effectively isolated, we could use the results to define a complete spectral model to be used to predict the ground shaking in the region. In order to compute the ground motions as a function of distance from the source for a range of different moment magnitudes, we needed a calibrated source model. We decided to use the Brune's model, combined with our results on the regional attenuation, the duration of the ground motions, and the absolute site response of sites.

Atkinson and Silva (1997) pointed out that the Brune spectral model consistently

over-predicted the ground motions for moderate-to-large events at low-to-intermediate frequencies (~ 0.1 - 2.0 Hz). They observed that the finiteness of the fault, even for moderate events, induces effects that may persist even at large distances from the source, and concluded that the finite-source effects could be the reason for the observed discrepancy between Brune's model simulations and the observed data.

AS2000 obtained a good agreement with California strong-motion data using the stochastic point-source simulation from the two-corner source spectrum, coupled to the Generic Rock Site amplification function, V(f), published by Boore and Joyner (1997). The high-frequency attenuation term, $\exp(-\pi\kappa_0 f)$, was also included (with κ_0=0.035 sec). For soil sites, the amplitudes predicted in AS2000 were modified from the rock ground motions using the empirical factors obtained by Abrahamson and Silva (1997). These are nonlinear, frequency-dependent soil amplification factors, which are also a function of the input peak-ground motion at bedrock. In the AS2000's spectral model, the low-frequency corner is related to the source size, whereas the high-frequency corner depends on the size of the sub-faults.

The functional form describing the regional attenuation used by AS2000 was taken from Raoof et al. (1999): a bi-linear geometric spreading with a cross-over hypocentral distance at 40 km, coupled to the regional attenuation parameter $Q(f)=180f^{0.45}$. The geometric spreading term is characterized by a body-wave-like decay ($\propto 1/r$) at short distances, and a surface-wave-like decay at larger distances ($\propto 1/\sqrt{r}$). The duration function used in AS2000 was also taken from Raoof et al. (1999): $T(r)=T_0 + 0.05r$ (r is the hypocentral distance in km; T_0 is the duration of the specific rupture).

Differences between the Brune source model, and the two-corner one are not very large for M<6. For M~5, in fact, the two spectral models yield results that are practically identical. In this paper we provide predictions for the ground motions up to M_w7 (Loma Prieta earthquake), by using: i) the classic Brune source model; ii) the generic rock site by Boore and Joyner (1997); iii) the high-frequency attenuation parameter κ_0=0.035 sec; iv) a static stress drop $\Delta\sigma$= 15 MPa. Predictions at the generic rock sites were convolved with relative transfer functions to get ground motions at different NEHRP site classes

We decided to use selected site responses taken from the literature, like the

Generic Rock Site by Boore and Joyner (1997), and the NEHRP site classes C and D. Predictions were initially computed for the Generic Rock amplification function, and attenuated with the parameter κ_0=0.035 sec, as recommended by Boore and Joyner (1997). Likewise, predictions for the NEHRP sites C and D were also obtained. For our reference site BRIB, we noticed that its absolute horizontal site terms were coincident, up to 2 Hz, with those of the Generic Rock.

Estimates of peak ground motions were computed for four events of M ≥ 5.8 that occurred in the extended Bay Area (PGA, PGV, and horizontal Spectral Accelerations, SA(f), f=0.33, 1.0, and 5.0 Hz, 5% damping). By modeling such a range of different quantities, we sampled the characteristics of the source spectrum in a relatively wide frequency band, between 0.33 Hz (where the lowest-frequency SA is computed), and 10-20 Hz, where the PGA is carried at short distances. Intermediate-to-high frequencies are sensitive to changes in the stress parameter, whereas low frequencies may be sensitive to the chosen spectral model (e.g., single- vs. double-corner frequency). Results are shown only for the largest one of these earthquakes: the Loma Prieta main shock (M7), and are comparable or equivalent for the other events. Only the Brune model was used in this study. However, we note that, for the Loma Prieta event, differences in the source model would be insignificant in the frequency range sampled in this study.

Figure 11 presents RVT predictions for NEHRP site classes C and D, plotted as thin and thick lines, respectively, for a M_W7 event. Open and solid symbols are used for observations of the Loma Prieta earthquake at sites classified as C and D, respectively. Predictions for rock and soil sites obtained from AS2000 are also plotted in Figure 11 for comparison. Observations are taken from the NGA Strong Motion database, which provides observed strong ground motions as a function of hypocentral distances (other metrics are also available in the NGA database). None of these stations are in common with the BDSN stations used to determine the ground motion formulae. In spite of the fact that all the parameters obtained in this study were from weak-motion observations, Figure 11 illustrates that the ground motion model calibrated in this study is capable of excellent results even when its predictive power is extrapolated to magnitudes well above the maximum magnitude included in the data set.

In the effective model used for the predictions, in order to match the peak and the

spectral values obtained form the regressions, a stress parameter $\Delta\sigma$=8 MPa was used between M_w 5.0 and 5.5, and $\Delta\sigma$=10 MPa was used for $5.5 < M_w < 6.0$. For the predictions at $6.0 \leq M_w \leq 7.0$, the stress parameter was increased to $\Delta\sigma$=15 MPa. The stress parameters at M_W 5.0 and 5.5 were obtained by fitting the excitation terms of Figure 5. For events of larger magnitudes, the stress parameters were calibrated by fitting peak ground velocity, peak ground acceleration, and spectral accelerations at three sampling frequencies, as shown in Figure 11 for the Loma Prieta earthquake. If a constant stress parameter was chosen at all magnitudes, say, 10 MPa, the excitation terms of events at M_W 5.0 would have been overestimated at high frequencies, whereas the high-frequency ground motions for the Loma Prieta event would have been slightly underestimated. The described calibration provided an effective model for the excitation and propagation of the ground motions in the extended Bay Area. The reader must be aware that none of the mentioned parameters has a physical meaning if extracted from the context, and that the entire effective predictive model makes sense only if taken as a whole.

In Figure 12 we plot the predicted horizontal spectral accelerations (in units of g), based on the results of this study. Lines marked M5,6,7-GR refer to our predictions for the Generic Rock, whereas lines marked M5,6,7-D are for the NEHRP site class D. Predictions were made for M_W 5, 6, and 7, at 20 and 50 km epicentral distance. Predictions from AS2000 (rock and soil sites, respectively) are plotted with thicker lines marked M5,6,7-AS-R, and M5,6,7-AS-S. We conclude that, for the spectral acceleration induced by a moderate earthquake of M_w5.0 on rock sites, the high-frequency shaking obtained using our predictive relationships would be significantly lower from the one obtained using AS2000. Even though, in the engineering practice, over-designing may be better than under-designing, for real-time applications like, for example, ShakeMap, predictions need to be as accurate as possible, and therefore more attention should be paid to carefully calibrate predictive relationships as low as M_W5, a magnitude level that is well within the range spanned by our data set.

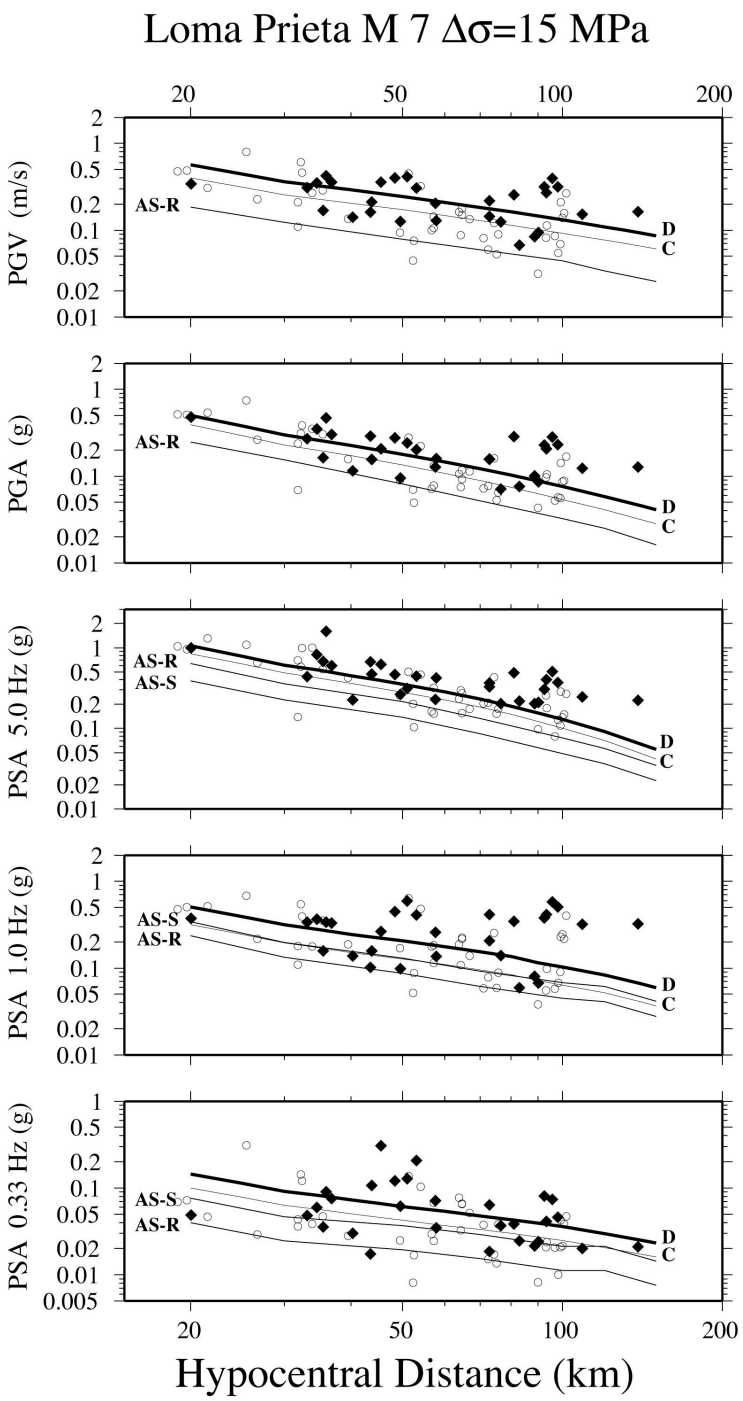

Figure 11 – Predictions of ground shaking for the M_w 7.0 Loma Prieta earthquake. Solid symbols are those from NEHRP class D sites, whereas clear symbols refer to measurements from NEHRP class C sites. Our predictions are shown as C (thin line) and D (thick line), whereas the ones from AS2000 are labeled AS-S and AS-R (soil and rock sites, respectively). Predictions are for: i) horizontal peak ground velocity (in m/s, top frame); ii) horizontal peak ground acceleration (second top frame, in units of g); iii) horizontal spectral accelerations at three reference frequencies (in units of g): 0.33 Hz, 1.0 Hz, and 5.0 Hz (bottom three panels). All our results were computed relative to the generic rock site term by Boore and Joyner (1997),

integrated with the high-frequency filter $\exp(-\pi\kappa_0 f)$, κ_0=0.035 sec.

Spectral Acceleration

In order to obtain a comparison between our predicted spectral acceleration terms (5% damping) and the observed data for a suite of events, we repeated the regressions on the observed spectral accelerations, at the same sampling frequencies used to obtain the results plotted in Figures 3-8. Figure 12a shows all the available excitation terms between M_w 4.0 and M_w 4.75 (left frame), and around M_w 5 (right frame), with the predictions obtained with the excitation/attenuation model proposed in this study. Moment magnitudes of the largest events of our data set (M_w 5.12, 5.13, and 4.81) are from Mayeda et al. (2005).

Both empirical and synthetic spectra of Figures 12a,b are adjusted to the site response of the Generic Rock Site defined by Boore and Joyner (1997). The events plotted using a thick line show an anomalous behavior at high frequency, and for this reason they are marked as "Low $\Delta\sigma$?" ones. None of the events in Figure 12a are from the Geysers geothermal field, a region known to have anomalous events, but actually from near stations SAO and MHC. Figure 12b displays a comparison between our spectral acceleration predictions for M_w 4 and M_w 5, with the ones produced by AS2000, showing the tendency of AS2000 to over-predict our results as magnitude decreases.

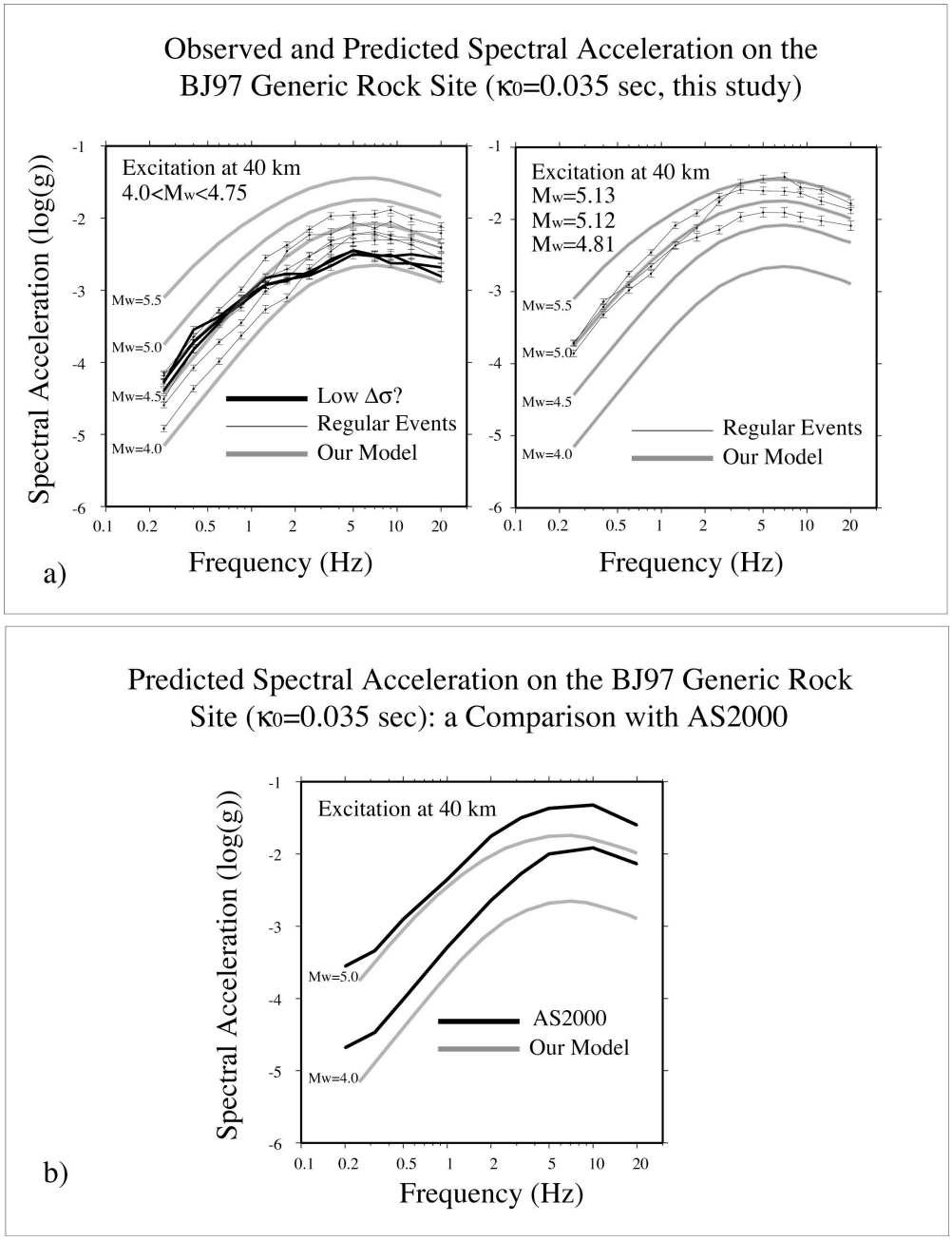

Figure 12 a) Left frame: empirical excitation terms (spectral acceleration) for events with $4.00<M_w<4.75$ (thin lines with error bars), adjusted to the Generic Rock Site by Boore and Joyner (1997), compared with theoretical predictions based on RVT and our excitation/attenuation model. All excitation terms are adjusted to the Generic Rock Site. Thick lines with error bars mark excitation terms with an anomalous spectral content (low stress-drop events?). a) Right frame: same comparison, for the excitation terms that are around M_w 5. b) Spectral acceleration synthetic excitation terms at 40 km hypocentral distance, M_w 4.0 and 5.0, computed using our model and the Generic Rock Site defined by Boore and Joyner (1997) (gray lines) and from AS2000 (black lines).

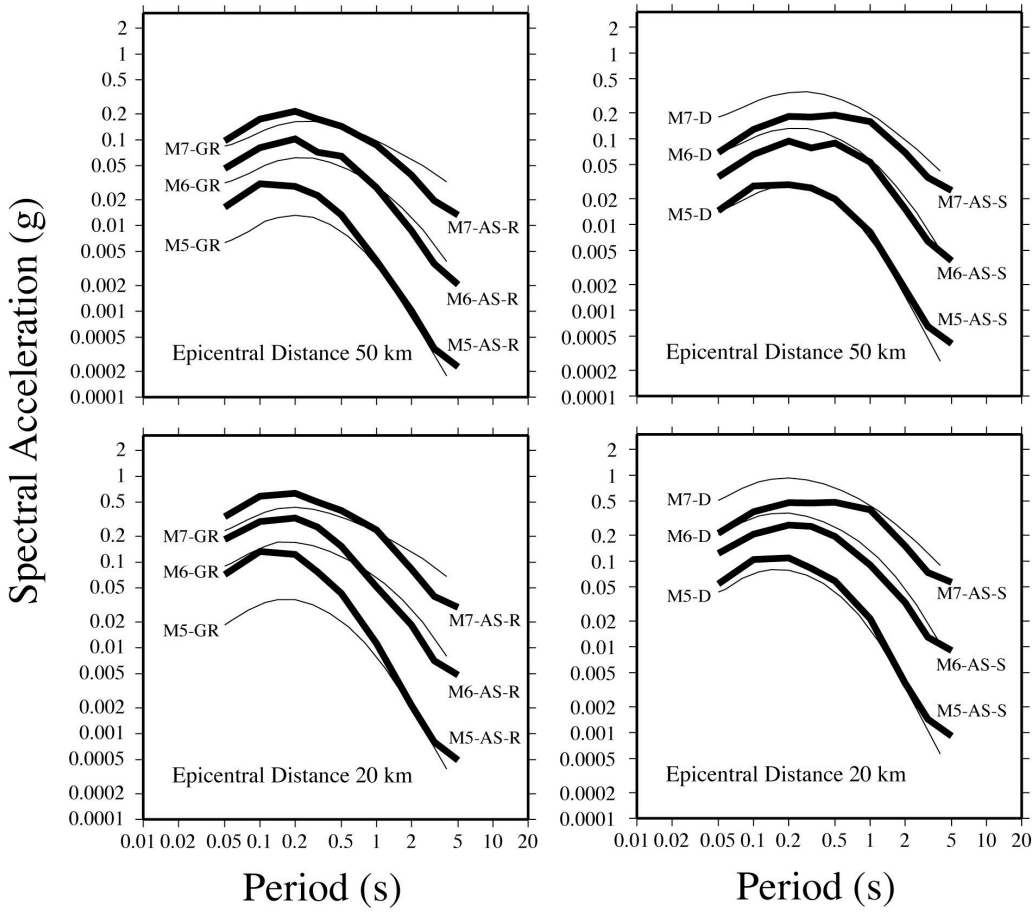

Figure 13 – Horizontal spectral accelerations predictions (in units of g), based on results of this study, are provided for the Boore and Joyner (1997) generic rock site (marked M5,6,7-GR), and for the NEHRP site class D (marked M5,6,7-D), for M 5, 6, and 7, at 20 and 50 km epicentral distance. For comparison, predictions from Atkinson and Silva (2000, rock and soil sites, respectively) are also plotted with thicker lines marked M5,6,7-AS-R, and M5,6,7-AS-S. The source model used for our predictions was the single corner Brune spectrum, with a magnitude-dependent stress parameter, 8 MPa at M5, 15 MPa at M6 and 7.

A more thorough comparison between the predicted values of spectral acceleration computed using our model and AS2000 is carried out in Figure 13, where are shown horizontal spectral accelerations predictions (in units of g), based on results of this study. Our predictions in Figure 13 are provided for the Boore and Joyner (1997) Generic Rock Site, and for the NEHRP site class D, for M 5, 6, and 7, at 20 and 50 km epicentral distance. For comparison, predictions from Atkinson and Silva (2000, rock and

soil sites, respectively) are also plotted.

Whereas in Figure 11 peak values are plotted as a function hypocentral distances, Figure 13 shows spectral acceleration as a function of epicentral distances. The use of these metrics is not an issue for small, shallow earthquakes and/or for large distances, since hypocentral, epicentral, and fault distances, all tend to the same value as they grow much larger than the fault dimensions. We can easily transform hypocentral distances to epicentral ones for point sources, and, for small events (our entire magnitude range), epicentral distances coincide to fault distances. AS2000 used the metrics: $R=\sqrt{d^2 + b^2}$, where d is the closest distance to the fault plane, and b≈5 at M_w≈5, and b≈14 for M_w≈8. However, predictive relationships based on epicentral distance are very important in near-real-time applications like ShakeMap, when we try to predict the ground motion in a region when the fault geometry responsible for a certain earthquake is still unknown. About ShakeMap applications, the electronic supplement provides a table of ground motion values (horizontal PGA, PGV, SA's at 0.3, 1.0, and 3.0 sec) to be used in such application for events up to M_w 5.0-5.5. The values in the electronic supplement are given, in MKS units, for a Generic Rock Site in the Boore and Joyner (1997) sense.

Discussion and Conclusions

The main purpose of this study was to provide a number of information/tools for the activities of seismic monitoring carried out by the Berkeley Digital Seismic Network around the San Francisco metropolitan area. Examples of these information/tools are: i) the absolute site terms for the Berkeley stations shown in Figure 7; ii) an automatic procedure to compute the M_W's shown in Figure 10; iii) a model to quantify the excitation/attenuation of the ground motion in the extended San Francisco Bay Area.

Whereas the usefulness of the M_W procedure may be obvious for the reader, a few words are needed in order to comment the value of the weak-motion-based predictive model for the ground motion that was developed in this study. In fact, the ability to correctly predict the earthquake-induced ground shaking in a wide magnitude range is crucial for a number of real-time applications like ShakeMap, which needs to produce accurate (not conservative) estimates of ground motion at all magnitudes, even at a moderate level (say, M_w between 3.0 and 5.5). This statement is especially true in regions

where the crustal attenuation is less than in the extended San Francisco Bay Area, where the building codes are less stringent than in California, and/or in areas where historical structures have not been retrofitted, and even the occurrence of an M_w~5 event creates a great deal of concern.

About the characteristics of the wave propagation in the study area, the geometric/anelastic parameters used to describe the regional attenuation around San Francisco are almost equivalent to what has previously been computed by Raoof et al. (1999) for Southern California. However, significant differences were found in the duration functions for the ground motions, which may be reflected into the predicted high-frequency amplitudes. Once the corrections for the regional wave propagation were obtained, we used independent estimates of the absolute source moment-rate spectra of all the events included in the regressions, and isolated the contributions of the site responses from the observed amplitudes. After a simple calibration procedure, we obtained ground motion predictions based on the Boore and Joyner's (1997) Generic Rock Site, and compared them against the results by AS2000. The same comparisons were carried out for the NEHRP site classes C and D. Differences between our results and the AS2000's predictions are probably due to the fact that our model is specific to a relatively small region, and this is not the case for AS2000.

The choice of the stress parameter to be used in the source term of our ground motion model is crucial. For earthquakes within the data set, up to M_W 5.13, the stress parameter was calibrated by matching the empirical source terms with the Brune spectral model. By matching the amplitudes of the synthetic ground motions on the available observations (PGA, PGV, PSA's at 0.33, 1.0, and 5.0 Hz), we also calibrated the Brune spectral model on four earthquakes of $M_W \geq 5.8$, including the M7 Loma Prieta earthquake, with the assumption that the recording sites stay linear during sustained, large shaking. We are certainly aware that the latter assumption may be questionable at short distances, and also that the distance metrics used (epicentral and hypocentral) may introduce other issues, but they are needed in real-time applications.

The predictive capabilities of our weak-motion-based model were tested outside and within the magnitude range of the original data set of calibration (our largest earthquake had M_w 5.13). Strong-motion predictions computed with our model were

compared against existing observations, as well as against strong-motion-based equations. As a representative example of the predictive equations that were produced for the region, we chose the work by Atkinson and Silva (2000), and used it as a reference. Comparisons with the results of different equations can be made in a relative sense.

Equations based only on strong-motion data from large events may be inadequate for predicting the ground motion induced by small events. In the ShakeMap context, for example, this issue is solved by deriving a specific predictive equation for small earthquakes in California. We stress the importance of the predictive capabilities for moderate-sized earthquakes, since the model by Atkinson and Silva (2000) (which is representative of an entire class of equations) tends to overpredict the shaking at M4 and 5 (see Figures 12 and 13).

For use in ShakeMap, a specific predictive relationship was developed for modeling the small events, through a multistage regression performed on data from hundreds of earthquakes in the magnitude range between M_w 3.0 and M_w 5.5, each recorded at many stations. The ShakeMap Small Regression (ShakeMap manual, p.148) is a modified form of the attenuation relationship for small events described in Wald et al. (1999), obtained on an extended version of the event database (to 2002). The Small Regression is used in ShakeMap as the default regression for events with magnitude below 5.3. For completeness of information, we must mention that, in northern California, the equation by Boatwright et al. (2003) is also implemented for both small and large earthquakes ("Large_seg" and "Small_seg" modules in the ShakeMap package). In the Electronic Supplement of this study we provide the information needed to implement our results into ShakeMap.

Finally, consistently with previous studies (e.g., Malagnini et al., 2004), the analysis on the absolute site terms of the BDSN showed that the main assumption on which the H/V method is based (i.e., the vertical motion is undisturbed, whereas site distortions affect only the horizontal motion) is not valid at most of the sites used in this study.

Electronic Supplements

The electronic supplements include the spectral accelerations at 0.3, 1.0, and 3.0 sec, the

peak horizontal velocity, and the peak horizontal acceleration, computed with our empirical model at each kilometer between 10 km and 200 km hypocentral distance, in the magnitude range between Mw 2.0 and Mw 5.5, every 0.1 magnitude units (file named: table_03.xyz, table_10.xyz, table_30.xyz, table_pgv.xyz. and table_pga.xyz, for PSA's at 0.3, 1.0, 3.0 sec, peak ground velocity, and peak ground acceleration, respectively). Scope of the supplements is the direct implementation of our results in the California's ShakeMap package. The Electronic Supplements are given in CGS units.

Acknowledgements

The thoughtful reviews done by Douglas Dreger and Mike Pasyanos, whom we wish to thank, strongly contributed to the clarity and the readability of this article. The authors are also grateful to Dave Wald and Bruce Worden, for some important discussions on the use of different predictive relationships within the ShakeMap package, and to two anonymous reviewers for their comments and criticisms.

L.M. and A.A. have been partially supported under project FIRB, Prot. RBAU013NRZ_001, funded by the Italian Ministero dell'Universita' e della Ricerca Scientifica (MIUR), and under project INGV-DPC (Dipartimento della Protezione Civile) S4 "*Stima dello scuotimento in tempo reale e quasi-reale per terremoti significativi in territorio nazionale*". Most figures were obtained using GMT (Wessel and Smith, 1991).

References

Abrahamson, N. A., and Shedlock, K. M. (1997). Overview, *Seism. Res. Lett.*, 68, 9-23.

Abrahamson, N.A., and W. Silva (1997). Empirical response spectral attenuation relations for shallow crustal earthquakes, *Seism. Res. Lett.*, 68, 94-127.

Akinci, A., L. Malagnini, R. B. Herrmann, R. Gok and M. B. Sørensen (2006). Ground motion scaling in the Marmara region, Turkey. *Geophys.l_J. Int.*, 166, 635 – 651.

Akinci, A., L. Malagnini, R.B. Herrmann, N.A. Pino, L. Scognamiglio, and H. Eyidogan (2001). High-Frequency Ground Motion in the Erzincan Region, Turkey:

Inferences from Small Earthquakes, *Bull. Seism. Soc. Am.*, 91, 1446 - 1455.

Atkinson, G. (1993). Notes on ground motion parameters for eastern North America: Duration and H/V ratio. *Bull. Seism. Soc. Am.,* 83, 587-596.

Atkinson, G. M., and W. Silva (2000). Stochastic modeling of California ground motions, *Bull. Seism. Soc. Am.* 90, 255-274.

Atkinson, G.M. and D.M. Boore (1997a). Some Comparisons Between Recent Ground-Motion Relations, *Seismological Research Letters*, Vol. 68, 24-40.

Atkinson, G.M. and D.M. Boore (1997b). Stochastic point-source modeling of ground motions in the Cascadia region, *Seism. Res. Lett.* 68, 74–85.

Atkinson, G.M. and W. Silva (1997). An empirical study of earthquake source spectra for California earthquakes, *Bull. Seism. Soc. Am.,* 87, 97 - 113.

Atkinson, G. M., and D. M. Boore (1995). Ground-motion relations for eastern North America, *Bull. Seism. Soc. Am.* 85, 17-30.

Baise, L.G., D. Dreger, and S.D. Glaser (2003). The effect of shallow San_Francisco Bay sediments on waveforms recorded during the M (sub w) 4.6_Bolinas, California, earthquake, *Bull. Seism. Soc. Am.,* 93, 465-479.

Boatwright, J., H. Bundock, J. Luetgert, L. Seekins, L. Gee, and P. Lombard (2003). The Dependence of PGA and PGV on Distance and Magnitude Inferred from Northern California ShakeMap Data, *Bull. Seism. Soc. Am.*,93, 2043 - 2055.

Boatwright, J., and G. L. Choy (1992). Acceleration source spectra anticipated for large earthquakes in northeastern North America, *Bull. Seism. Soc. Am.*, 82, 660 - 682.

Bodin, P., L. Malagnini, and A. Akinci (2004). Ground-Motion Scaling in the Kachchh Basin, India, Deduced from Aftershocks of the 2001 M_w 7.6 Bhuj Earthquake, *Bull. Seism. Soc. Am.*, 94, 1658 - 1669.

Boore, D. M. and W. B. Joyner (1997). Site amplifications for generic rock sites, *Bull. Seism. Soc. Am.*, v. 87, p. 327-341.

Boore, D. M., W. B. Joyner, and L. Wennerberg (1992). Fitting the stochastic ω^{-2} source model to observed response spectra in western North America: Trade-offs between $\Delta\sigma$ and κ, *Bull. Seism. Soc. Am.*, 82, 1956-1963.

Boore, D. (1983). Stochastic simulation of high-frequency ground motions based on seismological models of the radiated spectra, *Bull. Seism. Soc. Am.*, 73, 1865-1894.

Brune, J. N. (1970). Tectonic stress and the spectra of seismic shear waves from earthquakes, *J. Geophys. Res.* 75, 4997–5009.

Brune, J. N. (1971). Correction, *J. Geophys. Res.* 76, 5002.

Cartwright, D. E., and M. S. Longuet-Higgins (1956). The statistical distribution of the maxima of a random function, *Proc. R. Soc. London* **237,** 212-232.

Dreger, DS, and DV Helmberger (1990). Broadband Modeling of Local Earthquakes, *Bull. Seism. Soc. Am.*, 80 1162-1179.

Hanks, T. and R. McGuire (1981). The character of high-frequency strong ground motion, *Bull. Seism. Soc. Am.*, 71, 2071-2095.

Herrmann, R.B., and L. Malagnini (2005). Interpretation of High Frequency Ground Motion from Regional Seismic Network Observations, *Bull. Seism. Soc. Am.*, submitted.

Malagnini, L., K. Mayeda, A. Akinci, and P. L. Bragato (2004). Estimating absolute site effects, *Bull. Seism. Soc. Am*, 94, 1343-1352

Malagnini, L., A. Akinci, R. B. Herrmann, N.A. Pino, and L. Scognamiglio (2002). Characteristics of the Ground Motion in Northeastern Italy, *Bull. Seism. Soc. Am.,* 92, 2186-2204.

Malagnini, L. and R.B. Herrmann (2000). Ground-Motion Scaling in the Region of the 1997 Umbria-Marche Earthquake (Italy), *Bull. Seism. Soc. Am.,* 90, 1041-1051.

Malagnini, L., R.B. Herrmann, and M. Di Bona (2000a). Ground-Motion Scaling in the Apennines (Italy), *Bul. Seism. Soc. Am.,* 90, 1062-1081.

Malagnini, L., R.B. Herrmann, and K. Koch (2000b). Regional Ground-Motion Scaling in Central Europe*, Bull. Seism. Soc. Am.,* 90, 1052-1061.

Mayeda, K., L. Malagnini, W. S. Phillips, W. R. Walter, and D. Dreger (2005), 2-D or not 2-D, that is the question: A northern California test, *Geophys. Res. Lett.*, *32*, L12301, doi:10.1029/2005GL022882.

Mayeda, K., A. Hofstetter, J. O'Boyle and W. R. Walter (2003). Stable and Transportable Regional Magnitudes Based on Coda-Derived Moment-Rate Spectra, *Bull. Seism. Soc. Am.*, 93, 224-239.

Mayeda, K., S. Koyanagi, and K. Aki (1991). Site amplification from S-wave coda in the long Valley Caldera region, California, *Bull. Seism. Soc. Am.,* 81, 2194-2213.

Morasca, P., L. Malagnini, A. Akinci, and D. Spallarossa (2006). Ground-motion scaling in the western Alps, *J. Seism.,* in press.

Pasyanos, M., D. Dreger and B. Romanowicz (1996). Toward real-time estimation of regional moment tensors, *Bull. Seism. Soc. Am., 86*, 1255-1269.

Raoof, M., R.B. Herrmann, and L. Malagnini (1999). Attenuation and excitation of three-component ground motion in Southern California, *Bull. Seism. Soc. Am.,* 89,888-902.

Richter, C.F. (1935). An instrument earthquake magnitude scale, *Bull. Seis. Soc. Am.* 25, 1-32.

Schneider, J.F., W.J. Silva, and C. Stark (1993). Ground motion model for the 1989 *M* 6.9 Loma Prieta earthquake including effects of source, path, and site, *Earthquake Spectra* 9, 251-287

Scognamiglio, L., L. Malagnini, and A. Akinci (2005). Ground-Motion Scaling in Eastern Sicily, Italy, *Bulletin of the Seismological Society of America*, 95, 568-578; DOI: 10.1785/0120030124.

Silva, W.J. and R. Darragh (1995). Engineering characterization of earthquake strong ground motion recorded at rock sites. Palo Alto, California, *Electric Power Research Institute*, TR-102261.

Somerville, P. G., N. F. Smith, R. W. Graves, and N. A. Abrahamson (1997). Modification of empirical strong ground motion attenuation relations to include the amplitude and duration effects of rupture directivity, *Seism. Res. Lett.*, 68, 199-222.

Toro, G.R., N.A. Abrahamson, and J.F. Schneider (1997), Model of Strong Ground Motions from Earthquakes in Central and Eastern North America: Best Estimates and Uncertainties, *Seism. Res. Lett.*, 68, 41-57.

Toro, G.R., and R.K. McGuire (1987). An Investigation into Earthquake Ground Motion Characteristics in Eastern North America, *Bull. Seism. Soc. Am.*, 77, 468-489.

Uhrhammer, R. A., S. J. Loper and B. Romanowicz, Determination of Local_Magnitude Using BDSN Broadband Records, Bull. Seism. Soc. Am., 86, 1314-1330, 1996.

Wald, D. J., V. Quitoriano T. Heaton, H. Kanamori, C. W. Scrivner, and C. B. Worden (1999). TriNet ``ShakeMaps'': Rapid Generation of Instrumental Ground Motion

and Intensity Maps for Earthquakes in Southern California, *Earthquake Spectra*, 15, 537-556.

Wessel, P. and W. H. F. Smith, (1991). Free software helps map and display data, 72, 444-446.

Appendix 1

Table A1a

f_0 (Hz)	0.25		0.40		0.60		0.85		1.25		1.75		2.50	
R (km)	T(R) ± ΔT(R)		T(R) ± ΔT(R)		T(R) ± ΔT(R)		T(R) ± ΔT(R)		T(R) ± ΔT(R)		T(R) ± ΔT(R)		T(R) ± ΔT(R)	
15.000	9.868	0.593	11.931	0.539	11.469	0.434	9.877	0.345	8.369	0.280	6.764	0.243	5.271	0.218
20.000	12.674	0.461	14.696	0.400	14.384	0.320	12.078	0.255	9.421	0.208	7.602	0.180	5.774	0.162
30.000	15.480	0.480	17.461	0.416	17.300	0.333	14.279	0.262	10.473	0.213	8.441	0.184	6.277	0.164
40.000	18.286	0.475	20.415	0.429	20.215	0.333	17.576	0.258	12.917	0.208	9.279	0.179	6.779	0.160
50.000	20.333	0.507	23.369	0.458	22.293	0.341	16.847	0.263	11.973	0.213	8.913	0.182	6.427	0.163
60.000	22.380	0.534	24.372	0.472	21.861	0.346	16.118	0.266	11.476	0.216	8.547	0.185	6.091	0.166
70.000	24.427	0.525	23.617	0.435	21.429	0.318	15.389	0.243	10.979	0.196	8.328	0.169	6.088	0.151
80.000	25.230	0.563	22.862	0.445	20.998	0.322	15.511	0.245	10.873	0.195	8.790	0.168	6.922	0.150
90.000	26.032	0.560	22.106	0.426	20.566	0.312	16.417	0.237	13.596	0.191	10.417	0.164	7.827	0.147
100.00	26.834	0.551	21.351	0.373	20.782	0.267	17.323	0.202	13.812	0.163	10.897	0.141	8.052	0.128
120.00	25.991	0.641	24.383	0.440	23.969	0.305	18.313	0.227	14.172	0.182	11.435	0.158	9.387	0.146
140.00	25.147	0.827	27.415	0.528	27.156	0.353	21.751	0.255	16.989	0.202	13.881	0.175	11.257	0.164
160.00	24.304	1.401	30.447	0.914	30.343	0.584	25.190	0.406	19.807	0.317	16.327	0.272	13.127	0.255
180.00	23.461	2.420	33.479	1.829	33.530	1.318	28.628	0.987	22.625	0.787	18.774	0.678	14.996	0.619

Table A1b

f_0 (Hz)	3.50		5.00		7.00		9.00		12.5		17.5		20.0	
R (km)	T(R) ± ΔT(R)		T(R) ± ΔT(R)		T(R) ± ΔT(R)		T(R) ± ΔT(R)		T(R) ± ΔT(R)		T(R) ± ΔT(R)		T(R) ± ΔT(R)	
15.000	3.820	0.190	2.947	0.166	2.667	0.174	2.287	0.180	2.029	0.221	2.282	0.313	2.523	0.374
20.000	4.479	0.143	3.679	0.125	3.389	0.129	3.321	0.136	3.437	0.171	3.760	0.239	3.724	0.279
30.000	5.137	0.144	4.411	0.127	4.111	0.131	3.730	0.140	3.824	0.178	3.756	0.255	3.695	0.302
40.000	5.796	0.140	4.685	0.123	4.207	0.128	4.089	0.136	4.210	0.181	3.751	0.276	3.667	0.332

50.000	4.905	0.144	4.535	0.126	4.151	0.134	3.990	0.145	4.055	0.202	3.746	0.316	3.638	0.376
60.000	5.002	0.147	4.385	0.130	4.096	0.138	3.891	0.150	3.899	0.207	3.742	0.326	3.609	0.401
70.000	5.099	0.134	4.235	0.119	4.040	0.128	3.792	0.141	3.743	0.195	3.738	0.328	3.581	0.419
80.000	5.579	0.133	4.605	0.120	3.985	0.132	3.692	0.149	3.732	0.213	3.734	0.366	3.035	0.457
90.000	6.060	0.131	4.976	0.119	4.430	0.135	4.040	0.157	3.979	0.243	3.730	0.415	2.488	0.497
100.000	6.319	0.116	5.346	0.110	4.875	0.133	4.388	0.160	4.227	0.263	3.726	0.460	1.942	0.530
120.000	7.504	0.136	6.049	0.132	5.644	0.160	4.850	0.196	5.034	0.324	3.722	0.551	1.396	0.614
140.000	9.174	0.155	7.655	0.159	6.795	0.205	6.107	0.269	6.308	0.480	3.718	0.782	0.850	0.858
160.000	10.844	0.248	9.261	0.254	7.946	0.347	7.365	0.447	7.582	0.772	3.714	1.201	0.304	1.325
180.000	12.514	0.570	10.867	0.539	9.097	0.655	8.622	0.779	8.856	1.216	3.710	1.801	-0.242	1.990

Table A1a,b – Durations of the ground motions (the time window containing the 5% - 75% of the S-wave energy). The first column indicates the hypocentral distances at which the durations are computed. The empirical functions are indicated for every sampling frequency (L_1 estimate), together with the standard errors that are associated to each value (L_2 estimate). At the lowest frequencies, the empirical functions (piece-wise linear forms) strongly depend on the hypocentral distance, whereas signals at the highest frequencies tend to be characterized by constant durations. Durations are plotted in Figure 3.

Appendix 2

Station adjustments (δM_L) for the 12 stations in this study were calculated using a selected group of 16 local and regional earthquakes (Table A2.1) that were recorded by all three broadband components at all 12 stations between 2003/09/05 and 2004/12/15 and with an adequate signal-to-noise level (0.217mm < A < 890mm). The waveforms were deconvolved to ground motion and then convolved with the response of a standard Wood-Anderson (WA) torsion seismograph (Uhrhammer et al., 1996). The maximum trace amplitude (A, measured zero to peak in mm) for each synthesized WA (SWA) seismogram was then determined.

Table A2.1. Earthquakes selected for δM_L analysis.

Date	Time	Latitude	Longitude	Depth	M_L	Standard Error of the Mean
2003/09/05	01:39	37.84	-122.22	10.9	4.20	0.044
2003/09/25	14:33	36.82	-121.35	6.3	3.40	0.042

2003/10/24	22:00	36.70	-121.34	4.9	3.42	0.041
2003/11/06	22:04	37.21	-121.66	7.0	3.85	0.034
2004/01/31	02:11	37.10	-121.56	6.9	3.74	0.037
2004/03/16	06:38	36.81	-121.52	5.2	4.49	0.044
2004/04/29	19:49	37.73	-121.82	18.8	3.65	0.044
2004/05/04	17:25	36.70	-121.29	5.7	3.6	0.042
2004/08/30	04:30	36.58	-121.18	8.9	3.79	0.034
2004/08/31	09:12	36.59	-121.18	6.8	3.32	0.034
2004/09/22	10:57	36.80	-121.53	8.1	3.59	0.046
2004/10/25	19:55	36.97	-121.60	7.5	3.89	0.029
2004/11/01	22:02	37.07	-122.28	9.1	3.47	0.055
2004/11/24	02:06	36.61	-121.21	6.9	4.42	0.041
2004/11/24	05:23	36.60	-121.20	7.0	3.24	0.043
2004/12/15	04:16	36.64	-121.25	10.7	3.80	0.047

Once the SWA maximum trace amplitudes (A) were determined for each station/component (576 total observations), the local magnitude (M_L) was determined for each earthquake from the average of the individual horizontal component A's using the classic formulation of Richter:

$$M_L = \log_{10} A - \log_{10} A_o(\Delta),$$

where - $\log_{10} A_o(\Delta)$ is given analytically by:

$$- \log_{10} A_o(\Delta) = \log_{10}(0.3173 \exp(-0.00505 R) / R^{1.14}).$$

The δM_L for each component at each station is then determined from their respective mean residuals and the results are given in Table A2.2.

Table A2.2

Station Name	Component	Abs-Site $\pm\sigma$(Abs-Site)		$\delta M_L \pm \sigma(\delta M_L)$	
BDM	HHZ	0.22	0.11	-0.08	0.08
BDM	HHE	0.38	0.11	0.03	0.12
BDM	HHN	0.34	0.11	0.01	0.13
BKS	HHZ	0.13	0.08	-0.12	0.13
BKS	HHE	0.29	0.08	0.04	0.11

BKS	HHN	0.35	0.08	0.03	0.14
BRIB	HHZ	0.13	0.09	-0.11	0.12
BRIB	HHE	0.43	0.09	0.16	0.15
BRIB	HHN	0.36	0.09	0.07	0.12
BRK	HHZ	-0.11	0.10	-0.35	0.10
BRK	HHE	0.05	0.10	-0.14	0.12
BRK	HHN	0.05	0.10	-0.15	0.12
CVS	HHZ	0.08	0.12	-0.29	0.10
CVS	HHE	0.22	0.12	-0.12	0.12
CVS	HHN	0.15	0.13	-0.22	0.12
FARB	HHZ	-0.10	0.12	-0.37	0.11
FARB	HHE	0.03	0.11	-0.20	0.16
FARB	HHN	0.06	0.11	-0.19	0.15
JRSC	HHZ	-0.11	0.08	-0.25	0.12
JRSC	HHE	0.22	0.08	0.10	0.14
JRSC	HHN	0.12	0.08	0.04	0.14
MHC	HHZ	-0.13	0.08	-0.29	0.17
MHC	HHE	0.19	0.08	0.02	0.20
MHC	HHN	0.22	0.08	0.04	0.18
PACP	HHZ	-0.01	0.31	-0.24	0.17
PACP	HHE	0.41	0.32	0.23	0.18
PACP	HHN	0.41	0.32	0.18	0.14
POTR	HHZ	0.12	0.13	-0.18	0.13
POTR	HHE	0.45	0.13	0.07	0.11
POTR	HHN	0.45	0.13	0.08	0.11
SAO	HHZ	-0.01	0.09	-0.33	0.18
SAO	HHE	0.16	0.08	-0.19	0.18
SAO	HHN	0.15	0.08	-0.19	0.15
WENL	HHZ	0.28	0.09	0.02	0.15
WENL	HHE	0.43	0.09	0.13	0.14
WENL	HHN	0.46	0.09	0.19	0.14

Table A2.2. For each station used in this study, the table indicates the ML residual, with the corresponding error bar, and the corresponding absolute site term at 1.25 Hz, with its error bar.

Local Magnitude Adjustments (δM_L)

The average residual difference δM_L between the vertical (V) and the horizontal (H) components is –0.194 ± 0.076. Thus, +0.194 should be added to the δM_L(H) estimate to obtain the corresponding δM_L(V)estimate for comparison (Table A2.3).

Table A2.3

Station	δM_L(V)	Surface Geology
PAS	+0.394	Granite
BRK	+0.348	Franciscan Sandstone
FARB	+0.370	Granite
SAO	+0.325	Granite

Table A2.3. Average vertical component local magnitude adjustments at the stations sited on hard rock. PAS (Pasadena), located in a granite tunnel, which extends approximately 7 meters into a hillside in Southern California, is given for comparison because it was one of the original stations used in Richter's classic 1935 Local Magnitude paper.

The δM_L(V) for PAS, which is sited on granite, is comparable to the δM_L(V) values for the BDSN stations that are also sited on granite or hard rock. This implies that there is not a significant bias in the δM_L(V) values for northern and southern California. Using FARB as the reference station (because it is sited on granite) and assuming that δM_L(V)=+0.37 corresponds to Vs30 = 3300 m/s (the value for granite), the estimated Vs30 values for the 12 BDSN stations used in this study are given in Table A2.4.

Table A2.4

Station	δM_L(V)	Amp	Vs30 (m/s)	Bedrock
BDM	+0.084	0.52	1900	Sand
BKS	+0.122	0.56	2050	Claremont Cherts Shales
BRIB	+0.105	0.54	1980	Sandstone
BRK	+0.348	0.95	3170	Franciscan Sandstone

CVS	+0.290	0.83	2840	Tuff
FARB	+0.370	1.00	3300	Granite (reference station)
JRSC	+0.252	0.76	2640	Serpentine
MHC	+0.289	0.83	2840	Franciscan Graywacke and Greenstone
PACP	+0.223	0.71	2500	Miocene Volcanic Andesite
POTR	+0.180	0.65	2300	Eocene Marine
SAO	+0.325	0.90	3040	Gabilan Granite
WENL	+0.020	0.45	1670	Miocene Marine

Where it was assumed that the Vs30 value is proportional to ρVs and $\rho = 2.01 + 0.182$Vs (a variant of Birch's empirical relation). For Vs30 = 760, $\delta M_L(V) = -0.268$ which corresponds to a very soft alluvial site. For reference, the two softest sites, that were previously occupied by BDSN stations, are STAN and PKD1 which had $\delta M_L(V)$ estimated adjustments of -0.039 and -0.004, respectively. The average residual M_L difference between the V and H components is -0.194± 0.076 (excluding PACP which was not on the 1.25 Hz plot of Figure 9).